MINISTRY OF NATIONAL EDUCATION

THE ANNALS OF "DUNAREA DE JOS" UNIVERSITY OF GALATI

Fascicle IX

METALLURGY AND MATERIALS SCIENCE

YEAR XXXV (XXXX)
June 2017, no. 2

ISSN 1453-083X

2017
GALATI UNIVERSITY PRESS

Table of Contents

ANALYSIS OF THE FLOODS EFFECTS IN JUNE 2016 IN THE VORONET RIVER HYDROGRAPHIC BASIN

Mihail LUCA, Mihaela AVRAM, Nicolae MARCOIE
“Gheorghe Asachi” Technical University of Iasi, 63 Mangeron Dumitru Street, 770800, Iasi
e-mail: mluca2004@yahoo.com

ABSTRACT

The paper presents an analysis of the hydrological risk parameters registered in the Voroneţ river basin. The studies and researches took place on the Voroneţ River after the June 2016 floods. The research has taken into account the hydrological risk parameters of the last 20 years recorded in the Siret River Basin. The river basin of the Siret River has been affected by multiple floods in recent years. The floods have morphologically modified the minor and the major river Voroneţ, a situation that influenced the floodplain areas in the urban environment and outside. The research analyzed the precipitation, the liquid flows (minimum, average and maximum), the way of formation and evolution of the floods, the volume of the damage produced, etc. The investigation of the precipitation volume indicated a number of factors that have prevailed over the last 20 years. The precipitation value was 71.6 l/m^2 in two days. The flow recorded in the downstream section of the river was 118.12 m^3/s (the probability of calculation is 1%). The processing of liquid flow data revealed more flood flows in the same year. The effects of the floods have brought about the excessive degradation of shore defense works (about 2600 m) on the Voroneţ River located in the town of Gura Humorului, Voronet neighborhood and outside the city. The county road DJ 177D was degraded on 1600 m and two bridges were destroyed. Floods have resulted in the destruction of some economic and social objectives in the coastal area. The parameters of hydroclimatic risk highlighted by this research require special conditions for the design of works in the riverbed and the riparian area.

KEYWORDS: water scarcity, physical and apparent water losses, non-revenue water, pipe degradation

1. Introduction

Global climate changes are also present in Romania, where they have produced a number of direct influences on the hydrological cycle. The Romanian and Moldovan territories, in particular (the Siret and Prut basins), are situated in a hydroclimatic transition area characterized by more humid and moderately temperate ocean shades running from the western and continental regions with great thermal and pluviometric discontinuities, from the east [1, 2, 7].

At this stage there are changes in the annual distribution of precipitation and flows on hydrographic basins. The high value of the changes determines a significant hydroclimatic risk in the flow and river level evolution. Hydrological changes influence the behavior of existing buildings in the bed and riverine area [3].

The elements of hydrological risk affect the morphology of the minor bed, the stability of the bed constructions (bridges, regularization works) and the shore (shore defense works, dams). Hydrological risk elements affect the existing habitat in the minor and major river bed [1, 3].

Disastrous floods in recent years have caused significant degradation of the social and economic objectives of the riverside. The value of the damages has become very high, which requires large investments to be made for social and economic recovery. The effect of the changes can be immediately noticed or it occurs after a longer time [3].

The restoration of river regularization and river defense works depends directly on hydrological parameters. The disturbance of the hydrological parameters determines the behavior of the regularization works and, implicitly, the conditions of the river habitat.

2. Material and research method

The research area is situated in the river basin of the Voroneţ River, a tributary to the right of the Moldavian River. The hydrographic basin is located in the relief area of the Oriental Carpathians, in the geomorphological unit of the Stanişoarei Mountains (Figure 1). The altitude is 510-750 m and on average 730 m [10].

In the area there are a series of heights, called obcines, such as Obcina Voroneţ, Obcina Bătrânei, Obcina Brusturosului, Hill of Monastery, etc.

Fig. 1. *Physical map of the Voroneţ study area* [10]

The Voroneţ River has the cadastral code XII-1-40-26. The Voroneţ River presents a series of tributaries such as streams and torrents: on the left there are the streams Maghernita, Brusturos, Slătioara, and on the right the brooks Varniţa, Moara, Râla, Poiana, etc. (Figure 2). The Voroneţ River basin has an oval shape with a surface of 35 km^2. The length of the Voroneţ River is about 10 km and the slope of 3.17% [6, 8].

The research material consists of documentation and field studies, namely:

- Topographic studies to highlight the morphological changes of the river bed and riparian area.
- Hydrological studies for the determination of flood wave parameters and river flow.
- Hydraulic studies for highlighting the forms of motion and the parameters of the hydrodynamic erosion phenomenon.
- Geotechnical studies in the location of destroyed targets to determine the parameters that have affected the degradation phenomenon.
- Safety studies for the construction of buildings in the bed and the riparian area of the Voronet river, etc.

Some of the studies were taken from the literature and others were elaborated for the situation existing in the river basin. Research has been carried out at the site of the degraded areas and has been part of a technical expertise [4].

Fig. 2. *Location of Voroneţ river basin in the river hydrographic network of the Moldova river*

The theoretical and experimental research was carried out in the following domains [4]:

1. Research of hydrological parameters on the surface of the hydrographic basin considered in the study. Parameters analyzed are flows (liquid, solid), levels, frequency of floods, flood areas, etc.
2. Investigating the hydraulic parameters on the analyzed river section. Parameters analyzed are flows, levels, speeds, lengths and depths of erosion in the study sections located on the river.
3. Investigation of the hydrological risk parameters on the minor and major river bed morphology on the studied river sector.

4. Effect of risk parameters on structures and riverine habitat.

Primary data has been processed using statistical, hydrological, hydrological, resistance calculation software, applicable in this case study.

3. Results and discussions

The research was carried out on about 60% of the length of the Voroneţ River until it flows into the Moldavian River. The largest degradation of the bed and the riparian environment was recorded at this length. The sectors selected in the research are located in characteristic areas of the river basin as well as along the length of the river (Figure 3) and [4] respectively:

- Sector E1, the confluence of the Voroneţ River and the Slătioara brook (Camp Cristea area);
- Sector E2, the parallel route between the river and the county road DJ 171D;
- Sector E3, the confluence of the Voroneţ River and the Brusturos brook;
- Sector E4, Schit area;
- Sector E5, the parallel route between the river and the county road DJ 171D in the Voronet Monastery area;
- District E6, the urban area with degradation of the bridge and the riparian area;
- District E7, the intravilan area with riparian degradation.

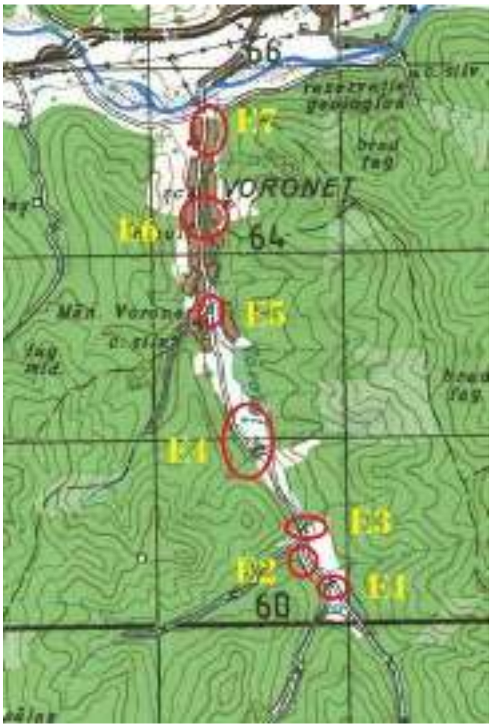

Fig. 3. *The location of the research sectors on the Voroneţ river* [4]

In the research we used climatic data taken from meteorological stations located in the analyzed river basin. Meteorological data were taken over varying time intervals (from 5 years to 45 years). Hydrological data were not collected because of the absence of hydrometric stations located on the Voroneţ River. The data from the hydroclimatic risk periods were analyzed by considering the data over a long period of time.

The Voroneţ River presents an ellipse-shaped river basin, which allows a rapid concentration of the flow (Figure 4). The erosive action of the water has made a minor bed with variable widths, where erosion, meandering and alluvial deposits occur. The river bed is characterized by intense morphological transformation over time.

For collecting data on the Voroneţ River, the meteorological station and the hydrometric station of the city of Gura Humorului were used. In May and June 2016 an abundant precipitation regime was recorded in the Voroneţ River Basin. The precipitations in the area with the highest value occurred during 18-20 of June. The values recorded at the Meteorological Station Gura Humorului were 71.6 l/m^2 [7].

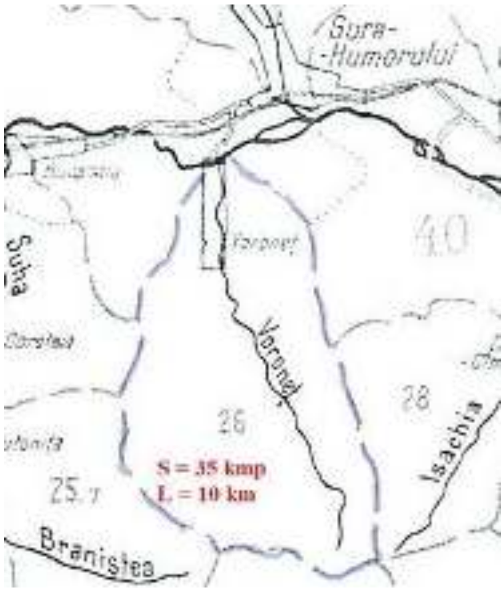

Fig. 4. *The Voroneţ River Basin* [6]

The Voroneţ River does not have a hydrometric station. Maximum flows were analytically determined. The maximum flow rate of 1% for hydrographic basins larger than 10 km^2 was determined by the rational formula [5]:

$$Q_{1\%} = \frac{K \cdot \alpha \cdot I_{60\ 1\%} \cdot F}{(F+1)^m} \qquad (1)$$

where: k = 0.28 is a rainfall transformation coefficient of mm / hour in m / s and the area in km^2 in m^2; α - global leakage coefficient; I60 1% - maximum hourly rainfall with 1% probability of exceedance; F - the area of the basin in km^2.

The parameter values in relation (1) were taken from [5] according to river basin characteristics. For the geographic area considered to have a surface area of 32 km^2, the values were: I60, 1% = 125 mm, α = 0.55, m = 0.49. From the calculations, the flow with 1% probability of calculation in the downstream area of the river, respectively Q1% = 118.12 m^3/s [4], was obtained.

The mean altitude of the river basin was 728 m (in the middle section it was 789 m) [4].

The Q1% flow rate was also determined in the middle section of the watercourse (Camp Cristea area), where the first degradations were recorded on the riparian buildings; the resulting value was 71.61 m^3/s. This flow was not fully taken over by the Voroneţ brook, aspect also revealed by the spills on the two banks, but also the important changes of the minor bed. The average multi-annual flow rate is 0.325 m^3/s.

The simulation and verification of flood flows on the Voroneţ River with the probability p = 1% for the flood in June 2016 are presented in Table 2.

Table 1. *Flow Q1% calculated and estimated on the Voroneţ River during the June 2016 flood* [4]

Nr. crt.	S (km^2)	Q_c (m^3/s)	Q_{sp} (m^3/s)	Q_{re}^* (m^3/s)
	36.0	118.12	141.74	130.0
	14.6	71.61	85.93	68.0
*- source ABA Bacău 2016				

The precipitations concentrated in a short period of time influenced the water flow in the Voroneţ basin. The floods caused by the Voroneţ River were intensified by the rapid discharge of the water from the slopes by torrential formations (eg. the Brusturosu stream). The concentration time was reduced by the circular / oval shape of the river basin.

The streams have carried alluvial material made of stone (medium and large dimensions), alluvium and forest material. The forest material was variable and even large, so the erosive effect on the bedside, bridges and shores was important. At the confluence and bridge areas there have been bottlenecks and narrowing. The blockages have led to discharges in the coastal area occupied by dwellings, agricultural land, sights, roads, etc. [1, 4].

Fig. 5. *General view of the Voroneţ River shore erosion at the limit of the road DJ 177D in the downstream area after the flood of June 2016 (photo Aug. 2016* [4]*)*

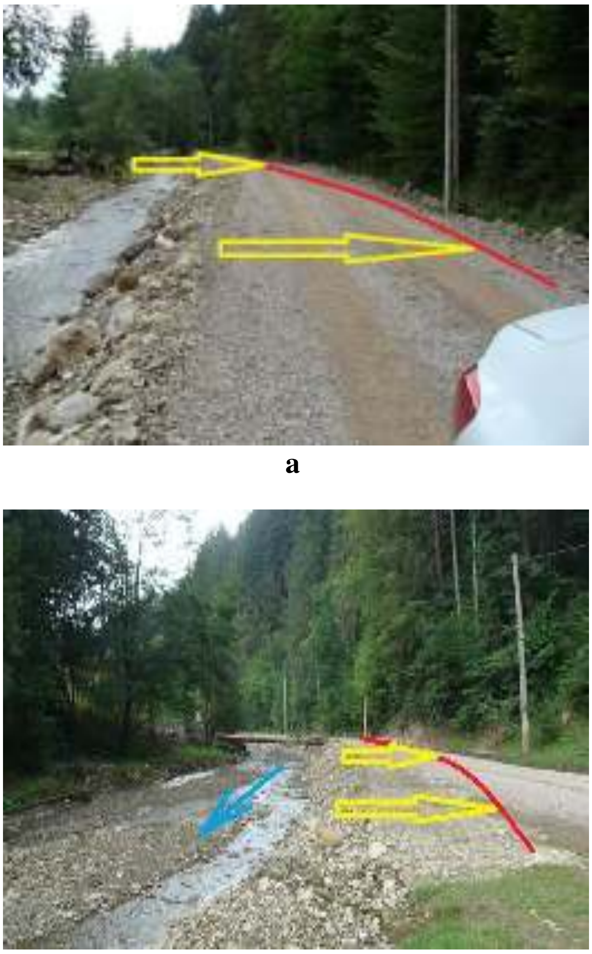

a

b

Fig. 6. *Details of the Voroneţ River's erosive action on the left bank and the road DJ 177D: a - the beginning of the deforestation degradation and the erosion of the road (downstream "Camp Cristea"); b - the end zone of the eroded road section to the slope (upstream of the Brusturos Brook)* [4]

The forestry and stone materials were carried outside the Voroneţ River bed and caused degradation phenomena of the riparian objectives (dwellings, agricultural land, tourist areas, water catchments, etc.). In some areas, the shore was eroded at depths of 2-5 m. A number of citizens' goods were taken by the floods from the bed and transported downstream [1, 4, 9].

The effects of the flood in June 2016 along the Voroneţ River are multiple. The most significant degradations are represented by the following [4]:

- structural degradation of the county road DJ 177D on a length of 1500 m and breaking it on a length of 400 m (Figure 5 and 6);
- partial and total degradation of the bridges (5 bridges), of the footbridges (17 footbridges) and of the pedestrian bridges along the river's length affected by the flood;
- the degradation of shore defense works in urban and out-of-town areas;
- the erosion of the bank in urban and out-of-town areas, a situation that affected individual riverine properties;
- the morphological modification of the river bed by sectors, with the change of flow paths;
- material and human losses.

The river banks were eroded (2600 m of shore) and the bed was morphologically transformed (Figure 5) [4, 9].

The county road DJ 177D was degraded on a route from the Voroneţ district to the "Camp Cristea" area. The county road is parallel to the Voroneţ riverbed on this route at distances of 1.0-45 m. The degradation forms are represented by the erosion of the marshalling with the entrance to the structure and its breaking on the differentiated length [4].

The county road was degraded to a length of 1500 m. High intensity hydrodynamic erosion led to the degradation of the road 177 177D, until its total destruction over a length of 400 m (Figure 6). This situation caused the interruption of traffic over a period of time. The river advanced to the shore, then into the road until it touched the slope (Figure 6.a). The phenomenon has been accelerated by the river's curvature area, the absence of shore defense and the geotechnical constitution of the land.

The reduced dimensions of the Voroneţ River flow section in the degradation area, as well as the absence of shore defense works, were the factors that allowed excessive road erosion. Old shore defense works have been degraded and no longer have a functional role in the transit of floods (Figure 5). The hydrodynamic erosion phenomenon of the bed has led to the lowering of the foundation quota of the shore defense constructions. The absence of rehabilitation works has led to a decrease in the protective capacity of shore defense works [3].

Fig. 7. *Detail regarding the Voroneţ River's erosive action on the river and the road in the Voroneţ Monastery area* [4]

a

b

Fig. 8. *Details of Voroneţ erosive action on the riverbed and its impact on the riparian area: a - bank erosion and damage to a dwelling construction; b - morphological modification of the bedrock with excessive erosion of the left bank* [4]

The reconstruction of the county road must be correlated with the design and execution of shore defense works on the affected river sector.

The section of the riverbed in the area of the Voroneţ Monastery has been affected by erosion phenomena, with an extension in the county road structure. Coastal defense works are degraded and aged without rehabilitation and upgrading. About 2.77 km of coastal defense were degraded by the flood of June 2016 [4].

The alluvial material (large stone, ballast, forest waste, etc.) driven by floods degraded the individual properties located in the river area (tourist hostels, dwellings, pedestrian bridges, agricultural land, etc.).

The degradation of the properties was favored by the non-observance of the law on the distances and the location of the constructions in the riparian area (Figure 8) [4].

The flood from the torrent Brusturos degraded the forest road on about 200 m, and the bridge at the confluence with the river Voroneţ was destroyed. The alluvial transport of the large stone-water mixture eroded the banks and the forest road.

The field analysis has highlighted the blocking of the section of the bridges, footbridges, pedestrian bridges, and small-scale areas. In this context, the transit of water and alluvial material was made over the bridge, the road and the neighboring areas of the minor and major beds.

The destructive phenomena have been of great intensity, over an important length of the river, and the damage is important and requires large investments for remediation.

Floods are a pollutant transport vector that transforms local pollution into regional and trans-regional pollution.

The analysis carried out in the Voroneţ river basin has revealed a number of hydroclimatic risk factors, namely:

- precipitation concentration on short intervals (1-2 days);
- the high frequency of torrential rainfall over short intervals (in the same month);
- reduced river bed capacity for floods with high flows;
- morphological modification of the river bed, erosion of the shore and shore, blocking of the bed, etc.;
- erosion zones adversely affect the stability of buildings and installations in the riverbed;
- increased transport of forestry material to the bedside because of uncontrolled deforestation.

4. Conclusions

1. The territory of the Voroneţ catchment area has been affected in the last 15 years by disastrous hydrological phenomena, which have significantly influenced the morphology of the riverbed, with important influences on the riverine environment. Flood damage has required large investment funds for rehabilitation.

2. During the period 2004-2017, a series of floods with high flow rates but also with high frequency at reduced intervals occurred in the Siret basin which caused morphological changes of the bed and degraded the regularization and shore defense works.

3. The floods produced in June 2016 on the Voroneţ River recorded flows with the probability of 1%, a situation that caused extremely destructive effects on the riparian area.

4. The Voroneţ river flow from June 2016 caused important degradations on the county road in the "Voroneţ Monastery" area, exemplified by the erosion of the bank and the road, as well as the damage of the coastal constructions.

5. The climatic phenomena produced in the Voroneţ river basin over the last 5 years can be characterized as hydroclimatic risk phenomena because of their destructive influence on the coastal area occupied by the dwellings, the county road and the morphology of the riverbed.

References

[1]. Avram M., *Research on the Impact of Hydroclimatic Risk Factors on the Design, Implementation Technologies and Operation of River Regeneration Works - Case Study*, Research report 2, "Gheorghe Asachi" Technical University from Iasi, 2016.

[2]. Luca M., Ignat A., *Morphological Changes Caused by Floods in 2004-2007 on Soci Area at the Moldova River*, International Conference „Disaster and Pollution Monitoring – IC.DPM. 3". 1-2 nov. Iaşi, I, p. 83-92, 2007.

[3]. Luca M., Stoenescu I., *Current Issues Concerning Regularization Works Behavior under Disaster Conditions*, International Conference „Disaster and Pollution Monitoring – IC.DPM. 3". 1-2 nov. Iaşi, p. 93-98, 2007.

[4]. Luca M., *Technical expertise "Reconstruction of shore defense at the Voroneţ brook, 600 m long (area Slevoacă and Monument), through works of gabion for safe construction of road DJ 177D, sector in the administration of Gura Humorului*. SC Polias-Instal Iasi, 2016.

[5]. Stăncescu L., Moraru N., Ionescu V., Leinweber L., *Technical guide for land improvement works*, Ceres Publishing House, Bucharest, 1984.

[6]. Ujvari I., *The geography of Romania's waters*. Edit. Scientific, Bucharest, 1972.

[7]. Vamanu E., Olariu P., *Hydroclimatic hazards in the Siret hydrographic area in the context of geographic changes*. Collection of papers, Annual Scientific Session INMH Bucharest, 2002.

[8]. ***, *Atlas of Water Cadastre in Romania*, Ministry of Environment, Bucharest, 1992.

[9]. ***, *Summary reports on flood protection, dangerous hydrometeorological phenomena, hydrotechnical accident and accidental pollution in Bacău County*, Siret Basin Water Administration, 2016.

[10]. ***, *The geographical Atlas of Romania*, Didactic and Pedagogical Publishing House, Bucharest, 1985.

THE ANNALS OF “DUNAREA DE JOS” UNIVERSITY OF GALATI
FASCICLE IX. METALLURGY AND MATERIALS SCIENCE
N°. 2 - 2017, ISSN 1453-083X

ANALYSIS TOOLS FOR SUSTAINABLE MANAGEMENT OF CELL PHONE WASTE FOR METALS RECOVERY

Anișoara CIOCAN
“Dunarea de Jos” University of Galati
e-mail: aciocan@ugal.com

ABSTRACT

A modern cell phone contains over 60 metals, combined physically or chemically and in some cases covered with various types of plastics, ceramics, etc. For recycling, each metal from the device needs to be analyzed individually. Some of these metals (copper, gold, silver, platinum, tin, yttrium, etc.) are valuable and their recovery is effective from the point of view of the economic benefits. Others (lead, cadmium, arsenic, mercury, etc.) are toxic and environmentally important. Certain metals are valuable but also toxic at the same time. In this study were identified and discussed a series of analysis tools specific to sustainable management of WEEE. Those applicable to recycling of mobile phones waste, operation which has as main objective the recovery of valuable metals, are the following: quantitative evaluation; potential income from the sale of recovered metals; eco-efficiency of recycling; recovery yield of metal; impact on the environment.

KEYWORDS: cell phone waste, recycling, metals, recovering

1. Introduction

Metals account for approximately 30% of the mass of a mobile phone. Most of them are in printed circuit board, the most important component of the mobile phone. A modern cell phone contains over 60 metals, combined physically or chemically and in some cases covered with various types of plastics, ceramics, etc. (Figure 1).

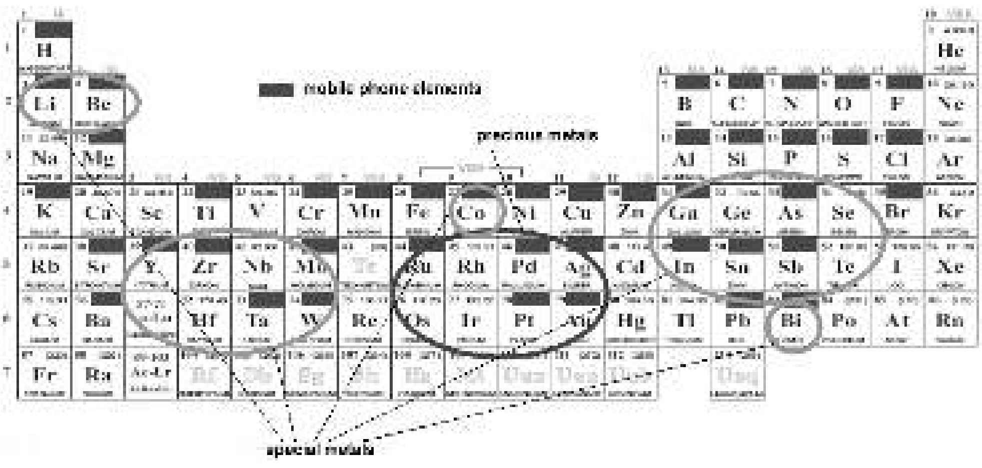

***Fig. 1.** Elements in mobile phone (source Nokia)* [1]

In general, the battery and accessories of a typical mobile phone contain: 43% plastic, 14% glass, 13% copper, 7% iron, 5% aluminum, 3% magnesium, 0.35% silver. Nickel, tin and lead are together about 1%, gold is less than 0.04% (276-446 ppm [2]), 0.1% antimony, < 0.02% palladium, < 0.01% beryllium and < 0.01% platinum (Figure 2).

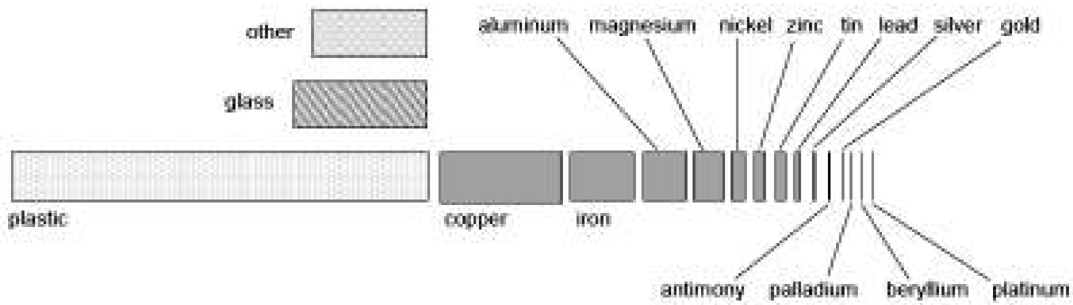

***Fig. 2.** Share of materials in the mobile phone (by weight)* [3]

Recycling end-of-life products is a key to achieving sustainable use of metals based on the number of products available for recycling [4]. Each metal from the electronic device needs to be analyzed individually to establish the opportunity and recycling potential. Some of these metals (copper, gold, silver, platinum, tin, yttrium, etc.) are valuable and their recovery is effective from the point of view of the economic benefits. Others (lead, cadmium, arsenic, mercury etc.) are toxic and environmentally important. Certain metals are valuable but also toxic at the same time.

2. Analysis of the sustainable recovery of metals from cell phones waste

By definition, sustainable materials management is an integrated approach toward managing material life cycles to achieve both economic efficiency and environmental viability [5]. The correct selection of metals for which recovery efforts and best recycling practices are justified can be done through management methodologies that are specific to sustainable management: substance flow analysis, product life cycle assessment, eco-efficiency, social integration [6].

The analysis of recycling opportunity focused on metals recovery must consider more indicators. Some are economic and others are related to environmental protection. Particularly for mobile phones waste, it is considered necessary to discuss about: quantitative evaluation; potential revenue from the sale of recovered metals; eco-efficiency of recycling; metal recovery efficiency; impact on the environment.

- Quantitative assessment of metals

This is a simplistic evaluation indicator of cell phone waste recycling process. This can lead to incorrect decisions regarding the metals present in small quantities. Most of them have significant economic and environmental potential [7].

Aluminum, iron, copper, cobalt, zinc, nickel, tin, chromium and lead are the main metals found in the mobile phone. The physical parameter, namely quantity, recommends the recovery of copper especially from the wiring and printed circuit board of the mobile phone.

- Potential revenue from the sale of recovered metals

Even if the quantitative physical parameter recommends the copper recovery from mobile phone waste, the value of precious metals (gold, silver and platinum metals) is the primary goal for recycling WEEE. The most famous precious metals are gold and silver. Also, in this group are included platinum metals: ruthenium, rhodium, palladium, osmium, iridium and platinum. In various contexts, plutonium and uranium are also considered precious metals.

The metal price represents a strong support for creating profitable recycling streams of WEEE (Table 1).

***Table 1.** Potential revenues from the sale of metals recovered from mobile phones waste* [8]

Metal	Metal recycled, [g/device]		Price of metal, [USD/g]		Value recovered, [USD/device]	
	with low yield	with high yield	2003	2006	with high yield at the price of metal from 2003	with low yield at the price of metal from 2006
Copper	8.84	14.85	0.0018	0.068	0.03	0.06
Silver	0.30	0.31	0.16	0.36	0.05	0.11
Gold	0.028	0.037	12.87	21.53	0.47	0.61
Palladium	0.012	0.019	6.53	10.61	0.13	0.13
Total	9.2	15.2			0.68	0.90

The benefit of metals recovery from cell phone is evaluated by intrinsic value (Table 2). This is given by multiplying the unit price by the metal concentration in the device [9].

It is noticeable that precious metals account for more than 80% of the total intrinsic value of metals recovered from a printed circuit board extracted from a piece of electronic waste although it represents only 1% (by weight) of the device mass.

Table 2. *Estimation of metals value from EEE used (for 2011)* [10]

Metal	World mine production, [t/a]	EEE demand, [t/a]	EEE demand/mine production, [%]	Metal price, [USD/kg]	Value of metals from EEE used, [billion USD]
Ag	22,200	7,554	34	649	4.90
Au	2,500	327	13	39,443	12.90
Pd	229	44	19	16,948	0.74
Pt	188	7	4	51,811	0.37
Ru	29	21	72	5,069	0.11
Cu	16,200,000	7,174,000	44	8	54.08
Sn	261,000	129,708	50	20	2.65
Sb	135,000	67,500	50	9	0.61
Co	88,000	16,470	19	45	0.75
Bi	7,600	1,216	16	20	0.02
Se	2,260	185	8	82	0.02
In	574	717	125	566	0.41
				Total	77.56

The electronic waste is considered valuable material (high grade material) compared to ores in terms of content in metals (Table 3). The value of electronic waste is given by the gold content. There are three classes of e-scrap: low value with < 100 ppm Au; medium value with 100-400 ppm Au; high value with > 400 ppm Au. The gold content of mobile phone wastes typically ranges from 100 to 400 ppm (in some cases it may exceed 400 ppm). In other types of electronic waste (TV-circuit boards and monitors, computers, etc.) the gold content can decrease below 100 ppm [12, 13].

Table 3. *Average content of metals in ores, in high-grade material and low-grade material* [11]

Content		Ores	High-grade material	Low-grade material
Fe	[%]	30-55	4.5-20	23-62
Cu		0.5-1.0	7-20	3.4-21
Al		25-30	1-4	1-10
Pb		0.5-15	0.3-6	0.2-1
Sn		<1	2.9-4.9	0.72-1.4
Au	[ppm]	5-7	16-566	10-20
Ag		5-7	18-1380	115-280
Pd		3-5	3-210	4-10

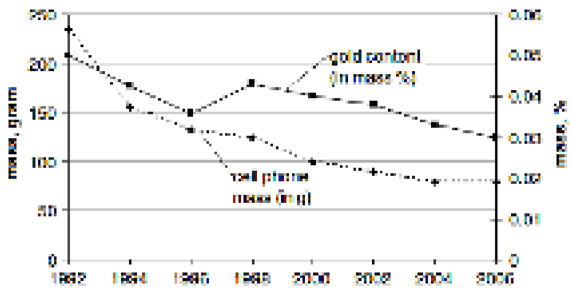

Fig. 3. *Evolution of gold content per mobile phone in relation to the average mass of the device between 1992 and 2006* [14]

Over time, as a result of the constructive evolution of mobile phones, the gold content per unit of product was reduced. For this reason, economic benefits given by proceeds from the sale of gold were decreased (Figure 3). Even so, the recycling of these pieces of equipment is still profitable.

The decreasing of the gold content was offset by the expansion of other metals recovery. In addition to gold, metallurgical refining technologies make it possible to recover palladium, silver, copper and a wide range of special metals such as In, Se, Te, Bi, Sb, etc. By recovering more metals, the gap created by gold is covered. Adding the values of silver, copper and palladium to gold value, over 95% from total revenues are obtained from cell phone recycling

(Table 4). In addition to silver, gold, copper and palladium from printed circuit boards, the cobalt recovering from Li-ion batteries is economically beneficial. The recovery of aluminum or magnesium alloys from the cases of cell phones is economically justified, too.

Table 4. *Value of recoverable metals from cell phones* [14]

Metal	Mass, [g]		Metal price in 2006, [cents/g]	Value of recoverable metals, [cents]	
	High	Low		High	Low
Ag	0.90	0.11	36.01	32.41	4.03
Al	7.20	1.52	0.27	1.94	0.41
Au	0.033	0.026	2151.71	70.15	56.12
Cr	0.72	0.20	0.82	0.59	0.16
Cu	20.68	9.30	0.68	14.09	6.33
Fe	6.62	2.70	0.10	0.66	0.27
Ni	2.74	0.70	2.43	6.64	1.70
Pb	0.80	0.28	0.17	0.14	0.05
Pd	0.09	0.00	1060.97	93.37	0.00
Sn	0.80	0.43	0.92	0.74	0.39
Zn	0.92	0.27	0.35	0.32	0.10
Total	41.57	15.56		221.03	69.56

- Eco- efficiency

This is another analytical tool characteristic of sustainable metals management. This has been launched by World Business Council for Sustainable Development in 1992. Eco-efficiency results from the combination of economic and environmental aspects and has the following objectives:

- the utilization of natural resources in the most efficient way;
- finding ways to reduce natural raw materials;
- identifying alternatives to replace the finite resources with renewable energy sources;
- reducing the negative impact on environment by using recycling solutions.

Maximizing the eco-efficiency of recycling is ensured by optimizing the environmental and economic balances.

This requires:

- maximizing metal recycling, minimizing environmental damage, taking into account the environmental footprint of the metal based on the quantities of saved natural resource, electronics waste not released in environment, CO_2 emissions;
- maximizing revenues from recycling materials, minimizing total recycling costs.

The total efficiency of recycling or the so-called recyclability of end-of-life products is determined by the weakest link of the recycling chain. For this reason, for EEE waste, the analysis should take into account the interdependencies between the stages of the recycling flow. This is the expression of the "concentration dilemma" or of the "degree of recovery" [15].

For the value generated by WEEE recycling but also for the toxicity control of process the following aspects are crucial: dismantling and pretreatment as well as the operations of final stage of waste processing, namely the metals recovery from fractions resulted from the mechanic processing (Figure 4).

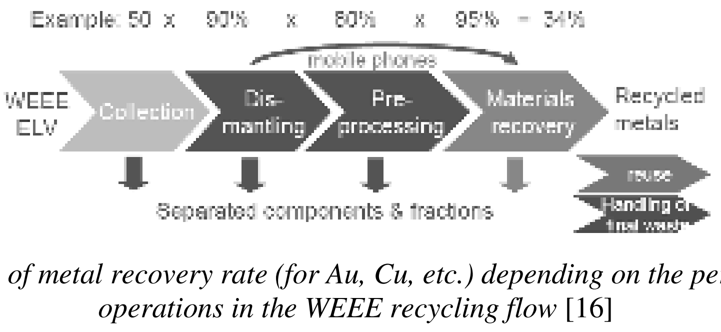

Fig. 4. *Efficiency of metal recovery rate (for Au, Cu, etc.) depending on the performance of the operations in the WEEE recycling flow* [16]

The eco-efficiency of WEEE recycling is directly related to an indicator named ″recovery efficiency of metals″. This reflects the impact of operations in the loop material recycling from the life cycle of product and represents the cumulative impact of several factors. The efficiency of the recycling process varies from metal to metal, depending on the material processed and the optimization degree of the process. Due to physical, chemical, thermodynamic and other limitations, the metal recovery rate will never reach 100%. As a complex function, the recovery efficiency of metals from WEEE depends mainly on two factors: the "collection rate" as a measure of the efficiency of the collection infrastructure; the "extraction yield of metal" as a measure of the efficiency of the metallurgical process focused on obtaining the desired quality of the metal.

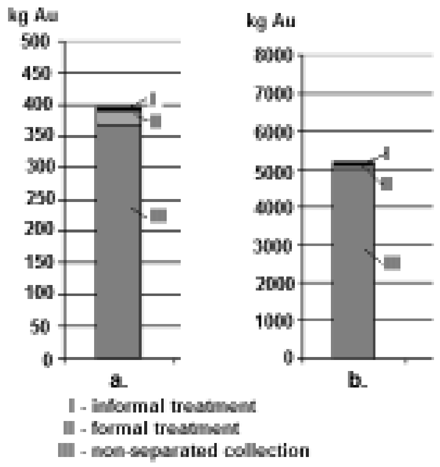

Fig. 5. *Quantity of the gold discarded and the source of the losses: Germany (a) and USA (b) in 2007* [17]

In many countries, the main step in the WEEE recycling stream in which precious metals are lost is the collection. The situation is particularly critical for mobile phone waste. Most of the metals are lost due to defective management, other losses being attributed to non-performing recycling treatments. For example, in Germany in 2007, the mobile waste collection rate was about 18% (not counting the hibernation equipment for the owners), and in the USA it was even lower, collecting only 11% of the equipment out of service, the others being eliminated most likely in the environment (Figure 5).

In practice, the metal recovery from mobile phone wastes ranges between 48 and 64% if the reporting is based on the total amount of metals contained in the equipment or between 12 and 19%, if the total mass of the equipment (including the battery) is taken into account. Unlike other categories of waste (automobiles, equipment and machinery from industrial applications, etc.), the recovery yield of valuable metals from electronic waste is still quite low: Ru 0-5%; Rh 5-10%; Pd 5-10%; Ag 10-15%; Ir 0%; Pt 0-5%; Ru 0-5%; Rh 5-10%; Pd 5-10%; Ag 10-15%; Ir 0%; Pt 0-5%; Au 10-15% [10].

Table 5. *Classification of elements based on the expression mode of the recycling rate (in accordance with Figure 6)* [10]

Interval	Element
Recycling rate expressed by percentage of metal in the end-of-life products that return to the manufacturing process of the new product: $EOL-RR=\frac{g}{d}x100$	
>50%	Al, Ti, Cr, Mn, Fe, Co, Ni, Cu, Zn, Nb, Rh, Pd, Ag, Sn, Re, Pt, Au, Pb
25-50%	Mg, Mo, Ir
10-25%	Ru, Cd, W,
1-10%	Sb, Hg
>1%	Li, Be, B, Sc, V, Ga, Ge, As, Se, Sr, Y, Zr, In, Te, Ba, Hf, Ta, Os, Tl, Bi, La, Ce, Pr, Nd, Sm, Eu, Gd, Tb, Dy, Ho, Er, Tm, Yb, Lu
Recycling rate expressed by the average content of the recycled metal (RC is the fraction of secondary metal in the total metal input of the production process $RC=\frac{(j+m)}{(a+j+m)}x100$)	
>50%	Nb, Ru, Pb
25-50%	Mg, Al, Mn, Fe, Co, Ni, Ge, Mo, Rh, Pd, Ag, In, W, Pt, Au, Hg
10-25%	Be, Ti, Cr, Cu, Zn, Ga, Cd, Sn, Sb, Ta, Re, Ir
1-10%	Se, Zr, La, Ce, Pr, Nd, Gd, Dy
>1%	As, Y, Ba, Os, Tl, Sm, Eu, Tb, Ho, Er, Tm, Yb, Lu
Share of post-consumer waste in the total waste recycled: post-consumer waste + manufacturing waste resulted from the recycling stream ($OSR=\frac{g}{(g+h)}x100$).	
>50%	Cr, Fe, Ni, Rh, Pd, Ag, Cd, W, Ir, Pt, Au, Hg, Pb
25-50%	Mg, Al, Mn, Co, Cu, Zn, Nb, Mo, Sn, Re
10-25%	Be, Ti
1-10%	Ru, Sb, Ta
>1%	Li, Ga, Ge, As, Y, In, Ba, Os, Ti, Bi

The comparative analyses for different metals or categories of waste should take into account the calculation method used to assess the recycling efficiency. Different values can be obtained because reporting can focus on the recovering of material, energy, or both material and energy, on resulting waste, etc. The results of the analysis performed on 60 metals confirm this hypothesis [10]. The calculating method of recycling rate changes the positioning of the metals in the five groups established: > 50%, 25-50%, 10-25%, 1-10%, <1% (Table 5).

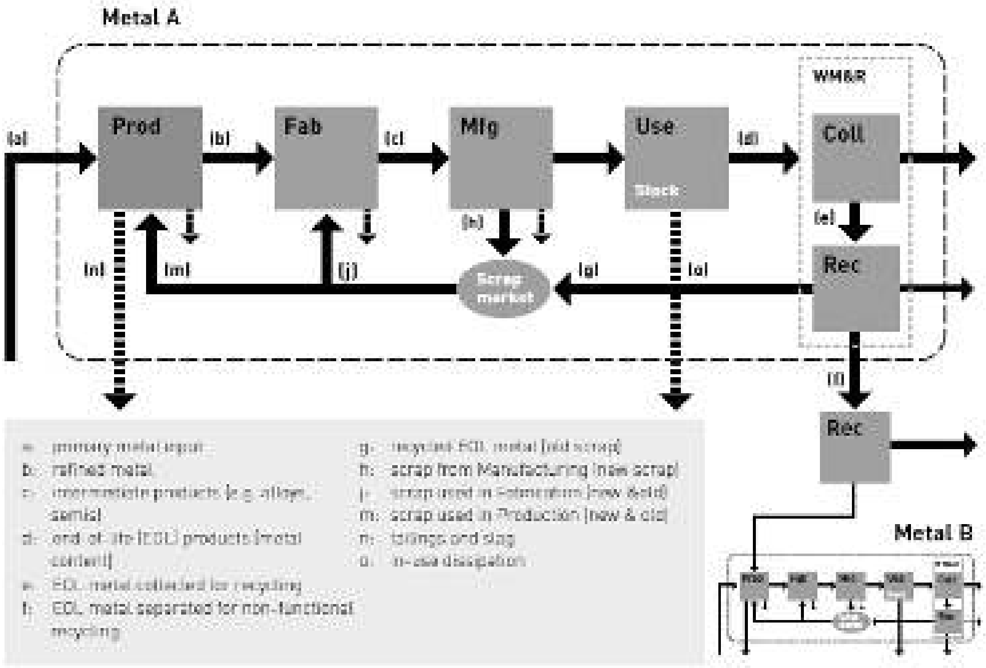

Fig. 6. *Stages of the life cycle of metals in EEE used to calculate recycling yields (Table 5)* [10]

It is noted that for many of the critical metals, especially rare earths, but also for other metals (such as tantalum, gallium and indium), the quantity returned from waste in the manufacturing process of new products is less than 1%. The status of precious metals (platinum, palladium, gold, silver) and cobalt is significantly better, reaching more than 50%. The situation is justified by the existence of efficient recycling technologies and by performant working of the collection systems for the recovered equipment.

- Environmental impact

WEEE recycling reduces the volume of waste damped, attenuates and prevents the pollution of soil, groundwater and air due to the release of hazardous compounds. The treatment of WEEE for metal recovery is mainly important for reducing the ″emissions of greenhouse gas″. Together with the ″material footprint″, the ″carbon footprint″ is one of the most important environmental targets for the recovery of metals from electronic waste.

The energy consumption (electricity, fossil fuels, non-conventional energy) is the indicator that characterizes the eco-efficiency which has influence on the amount of greenhouse gases of a process. Although energy consumption has an important share in the cost of recycling, the recycling processes are less energy intensive than primary metal production (Table 6). The energy consumed for extracting precious metals (gold, silver and palladium) is higher than the energy used for the production of basic metals (Cu, Al, Ni, Sn, Zn, Fe) (Figure 7).

Table 6. *Economic benefits of recycling some metals from the printed circuit boards, expressed by energy consumption* [19]

Material	Energy savings over virgin materials (%)
Aluminum	95
Copper	85
Iron and steel	74
Lead	65
Zinc	60

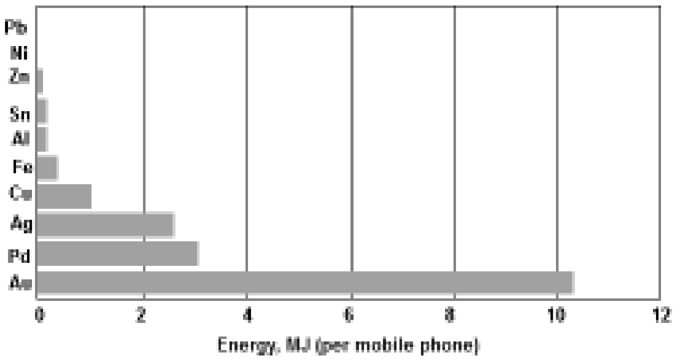

Fig. 7. *Energy consumed for extracting metals necessary for mobile phone manufacturing* [20]

The energy requirements for mining and extraction of raw materials are approx. 7% of the total global energy consumption. The large amount of energy required for the production of primary metals from ores is due to the high level of CO_2 emissions. The energy required for the mining production (extraction and the preparation of ores) is most often obtained from the coal burning. As a result, the environmental impact over the entire life cycle of metals is high. The impact of the production of metals from platinum group is shown in Figure 8.

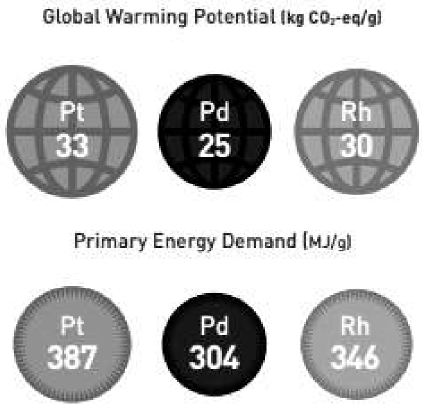

Fig. 8. *Summary result of the life cycle impact assessment for the average production of 1 gram of metals from platinum group* [21]

The extent to which mining and extraction activity affects the environmental factors differs from one metal to another. The metal-induced problems related to eco-toxicity are in close interdependence with the energy required to obtain the metals from ores (Figure 9). Depending on the magnitude of environmental effects, the rare metals are positioned at the top of the ranking.

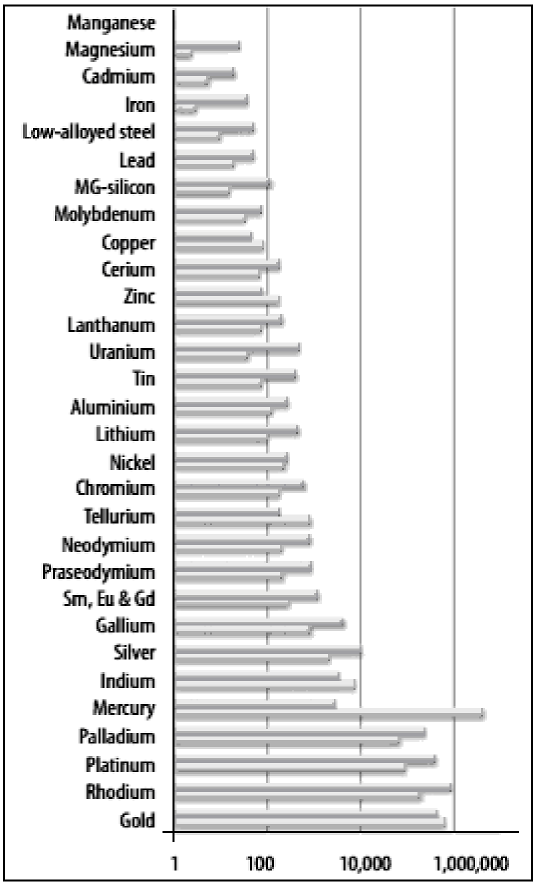

Fig. 9. *Contribution of metals to terrestrial ecotoxicity assessed by greenhouse gases and global warming for 1 kg of primary metal (for each metal the upper value is the greenhouse gases quantity and the lower is the terrestrial toxicity)* [22]

The literature data confirms that the production of primary metals from ores is an important source of CO_2 emissions. In this regard, even metals found in smaller amounts in EEE have a great impact on the environment (Figure 10).

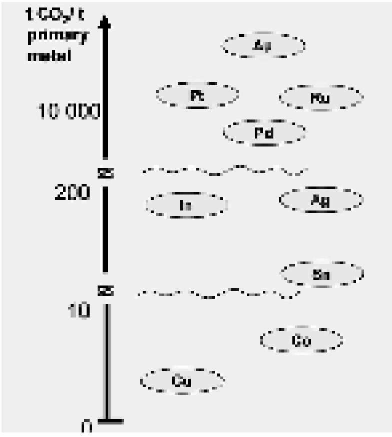

***Fig. 10.** CO_2 emitted by 1 t of primary metals production* [1]

For 1 kg of primary copper, nearly 4 kg of CO_2 is emitted [23]. When comparing emissions per unit of metal produced, the typical CO_2 footprint for 1 ton of gold is 5,000 times higher than for 1 ton of copper. But obviously, with more copper being produced, the copper industry annually releases about 1.3 times CO_2 compared to gold production.

The recycling of metals requires far less energy than primary production, often this is consumed only for re-melting. As a result, CO_2 emissions from recycling are substantially lower than those from mining and extraction of primary metal. For example, besides the huge reduction of energy consumption, the aluminum recycling generates only 5% of the amount of CO_2 than those emitted from bauxite ores production (if electrolysis is also taken into account). For 1 kg of recycled aluminum, only 1/10 of the energy required for primary production is consumed. Thus, the generation of red sludge (~1.3 kg) and the emission of CO_2 (~2 kg) can be prevented. The situation is the same for platinum metals and other metals recovered from WEEE (Figure 11) [10, 23].

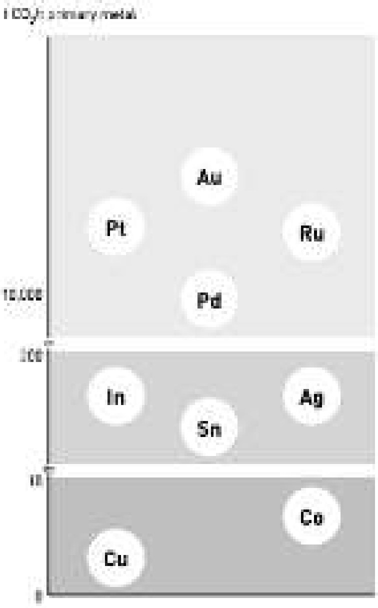

Metals used in EEE	Primary production intensity t CO_2/t metal	Demand for EEE t/a	CO_2 emissions Mt/a
Au – Gold	16,991	327	5.56
Pt – Platinum	13,954	8	0.11
Ru – Ruthenium	13,954	16	0.22
Pd – Palladium	9,380	30	0.28
Au – Silver	144	4,917	0.71
In – Indium	162	717	0.10
Sn – Tin	16	129,708	2.09
Co – Cobalt	8	16,470	0.13
Cu – Copper	3	7,174,000	24.39
		CO_2 total [Mt/a]	33.58

***Fig. 11.** Primary carbon footprint for some WEEE elements* [10]

The recycled gold has a smaller carbon footprint than the primary gold from ores. Although there are small amounts of gold in WEEE, this element has the largest footprint, i.e. is about 50 times larger than for copper and about 5000 times larger for aluminum [22].

3. Conclusions

The opportunity and recycling potential resulted from the analysis of each metal from cell phones waste. The indicators considered for sustainable recovery of metals are: quantitative evaluation; potential revenue obtained from recovered metals sale; eco-efficiency of recycling; metal recovery efficiency; impact on the environment. The quantitative evaluation of metals is an incorrect tool to develop sustainable materials management in case of mobile phones waste. The potential revenue obtained from the sale of recovered metals is the most important drive force for sustaining profitable WEEE recycling industry. In terms of metals value, the electronic waste is classified as ″high grade material″. The values of gold, silver, copper and palladium represent over 95% from the total revenues obtained by recycling cell phones waste. Another analytical tool characteristic of sustainable metals management is eco-efficiency. This is expressed by the extraction metal yield from waste. The low recovery yield of valuable metals (Ru 0-5%; Rh 5-10%; Pd 5-10%; Ag 10-15%; Ir 0%; Pt 0-5%; Ru 0-5%; Rh 5-10%; Pd 5-10%; Ag 10-15%; Ir 0%; Pt 0-5%; Au 10-15%) is characteristic of the electronic scrap. The quantity returned from waste in the manufacturing process of new products is less than 1% for many of the critical metals, especially rare earths, but also for other metals (such as tantalum, gallium and indium). The status of precious metals (platinum, palladium, gold, silver) and cobalt is significantly better, reaching more than 50%.

In terms of environmental impact, the eco-efficiency is quantified by greenhouse gases emission, material footprint or carbon footprint. Among metals in WEEE, gold and platinum metals are the most important source of CO_2 emission. The typical CO_2 footprint for 1 ton of gold is 5,000 times higher than for 1 ton of copper.

References

[1]. Hagelüken C., Meskers C., *Mining our computers – opportunities and challenges to recover scarce and valuable metals from end-of-life electronic devices*, In: Proc. Electron. Goes Green 2008+, Berlin, p. 623-628, 2008.

[2]. Morley N., Eatherley D., *Material Security Ensuring Resource Availability for the UK Economy*, C-Tech Innovation Ltd; Resource Efficiency, London 2008.

[3]. Hagelüken C., *Study to test the recycling guideline*, Mobile Phone Partnership Initiative (MPPI), 2008.

[4]. Hagelüken C., *Recycling of precious and special metals*, Eco-Efficiency in Industry and Science, Springer Science, p. 221-241, 2013.

[5]. Fiksel J., *A Framework for Sustainable Materials Management*, JOM, 2006.

[6]. ***, *Materials Case Study 1: Critical Metals and Mobile Devices*, Working Document OECD Environment Directorate, OECD, 2010.

[7]. Ongondo F. O., Williams I. D., Cherrett T. J., *How are WEEE doing? A global review of the management of electrical and electronic wastes*, Waste Management 31, p. 714-730, 2011.

[8]. Mangold J. A., *Evaluating the End-of-Life Phase of Consumer Electronics: Methods and Tools to Improve Product Design and Material Recovery, A dissertation submitted in partial satisfaction of the requirements for the degree of Doctor of Philosophy*, University of California, Berkeley, 2013.

[9]. Hagelüken C., Meskers C., *Technology challenges to recover precious and special metals from complex products*, http://ewasteguide.info/files/Hageluecken,_2009.

[10]. Reuter M. A., Hudson C., Van Schaik A., Heiskanen K., Meskers C., Hagelüken C., *Metal Recycling: Opportunities, Limits, Infrastructure, A Report of the Working Group on the Global Metal Flows to the International Resource Panel*, UNEP, 2013.

[11]. Havlik T., Orac D., Berwanger M., Maul A., *The effect of mechanical–physical pretreatment on hydrometallurgical extraction of copper and tin in residue from printed circuit boards from used consumer equipment*, Minerals Engineering, 65, p.163-171, 2014.

[12]. Hagelüken C., *Recycling of Electronic Scrap at Umicore's Integrated Metals Smelter and Refinery*, World of Metallurgy-Erzmetall, 59, no. 3, p. 152-161, 2006.

[13]. Evans C., Renz R., McCullough E., Lawrence S., Pavlenko N., Suter S., Brundage A., Hecht J., Lizas D., Bailey P., *Case Study on Critical Metals in Mobile Phones. Final Report*, http://www.oecd.org/env/waste/smm-casestudies.htm.

[14]. Geyer R., Doctori Blass V., *The economics of cell phone reuse and recycling*, Int J Adv Manuf Technol, 47, p. 515-525, 2010.

[15]. Hagelüken Ch., *Improving resource recovery from electronic scrap recycling - a holistic approach*, http://ieeexplore.ieee.org/iel5/10977/34595/01650064.pdf.

[16]. Hagelüken C., *Metal Recovery from e-scrap in a global environment. Technical capabilities, challanges and experience gained*, 6th session of OEWG Basel Convention, 2007.

[17]. Huisman J., Magalini F., Kuehr R., Maurer C., Delgado C., Artim E., Stevels A. L. N., *Review of Directive 2002/96 on Waste Electrical and Electronic Equipment (WEEE), Final report, United Nations University, for the European Commission*, Contract No. 07010401/2006/442493/ETU/G4, United Nations University, Bonn, Germany, 2007.

[18]. Cui J., Forssberg E., *Mechanical recycling of waste electric and electronic equipment: A review*, Journal of Hazardous Materials, B99, p. 243-263, 2003.

[19]. ***, *The Life Cycle of Materials in Mobile Phones. How New Phone Technology Affects the Environment*, 2014.

[20]. ***, *The Life Cycle Assessment of Platinum Group Metals*.

[21]. ***, www.unep.org/resourcepanel/Portals/24102/PDFs.

[22]. Tuncuk A., Stazi V., Akcil A., Yazici E. Y., Deveci H., *Aqueous metal recovery techniques from e-scrap: Hydrometallurgy in recycling*, Minerals Engineering, 25, p. 28-37, 2012.

[23]. Anindya A., *Minor Elements Distribution during the Smelting of WEEE with Copper Scrap*, Thesis PhD, School of Civil, Environmental & Chemical Engineering Science, Engineering & Technology (SET) Portfolio RMIT University, 2012.

THE ANNALS OF "DUNAREA DE JOS" UNIVERSITY OF GALATI
FASCICLE IX. METALLURGY AND MATERIALS SCIENCE
N°. 2 - 2017, ISSN 1453-083X

ANALYSIS OF THE PERFORMANCE COEFFICIENT OF THE ENERGETICAL RECOVERY OF THE DOMESTIC WASTE

Emanuel IACOB, Mariana-Florentina STEFANESCU, Alexandru DOBROVICESCU
Faculty of Mechanical Engineering and Mechatronics, University POLITEHNICA of Bucharest
e-mail: adobrovicescu@yahoo.com

ABSTRACT

The paper critically analyses the way of defining the coefficient of performance of the systems used for the recovery of the energy of the domestic waste in cogeneration plants. The R1 criterion of performance of the European Waste Framework Directive (2008/98/EC) is taken as a basis for the discussion.

The philosophy of establishing the form of the coefficient of performance depending on the definition of the system "Product" and "Fuel" is discussed.

It is pointed out the fact that the performance criterion R1 is established on an energetic basis that makes it insensitive to climacteric changes.

To take into account the interaction of the system with the environment in which it operates, the paper aims at defining a coefficient of performance based on the exergy concept that would make evidence of both the quantity and quality of the processed energies.

KEYWORDS: energetic recovery, municipal waste, coefficient of performance

1. Introduction

The correct estimation of the coefficient of performance of a system or piece of equipment is of a capital importance that makes possible to point out, for the given system, the possibilities of improvement of its operating mode and construction.

When one considers that a system operates better than it really does, opportunities of improvement are lost. On the contrary, when a system is considered weaker than in reality, one will focus his attention on trying to improve its characteristics – efforts made in vain because the system was operating well.

What one expects from a system, called the system Product, represents its net output that another system or subsystem is interested to buy [1].

From an economic point of view, the Product represents the result of an activity that is sold by a subsystem and purchased by other subsystems.

The Fuel represents the net resource that a system consumes to accomplish the final product.

The efficiency of any subsystem or system as a whole is given by the ratio between Product and Fuel.

The correct estimation of the generic Fuel and product of each operating zone is the key action for a proper evaluation of the local and finally global efficiency of the system, pointing out possibilities for the improvement of the system operating and design [2].

2. The R1 criterion for assessing the efficiency of the energy recovery of the municipal solid waste

The package of good practice of the European Community regarding the municipal solid waste management, part of the Waste Framework Directive (2008/98/EC), introduces the R1 criterion depending on which any system of waste processing could be rated as an energy recovery system or as an incineration facility [3].

The relation for calculating the Coefficient of Performance of a municipal solid waste energy recovery system wants to account not only for the system efficiency taken on its own, but also for the way the energy recovered is used.

The R1 criterion is:

$$R1 = \frac{E_p - (E_f + Ei)}{0.97(E_{mw} + E_f)} \geq \text{ Limit} \tag{1}$$

where the Limit from which a system for processing the municipal waste could be considered an energetic recovery system is for the existing installations and for the systems starting the operation after adopting the Waste Framework Directive (2008/98/EC).

The terms in equation (1) have the following significance:

- energy produced annually as electricity or heat [GJ/y];

- annual consumption of energy with the conventional combustible necessary for producing process steam [GJ/y];

- it represents complementary energy different from an energy that does not contribute to the producing of process steam;

- the annual energy contained in the processed waste, calculated based on the Low Heating Value (LHV) [GJ/y].

3. Discussions on defining the Coefficient of Performance of a system for the energy recovery of the municipal solid waste

To understand the significance of the terms in Eq. (1) the Product and the borders of the system should be stated. Dealing with an energetic analysis, the observer is situated out of the system borders and accounts only for the energetic interactions by mass and energy transfer between the system and its surroundings.

The installation for the energetic recovery of the municipal waste produces process steam, electrical energy and heat, making use of a steam turbine system.

Figure 1 shows the schematic of the energy balance of the combined system made of the incinerator and the steam turbine for the energy recovery from the municipal solid waste.

The energy balance equation for the combined system becomes:

$$\begin{aligned} E_f + E_{mw} + E_f^{com} + E_{com} + E_{el}^i &= \\ = E_{el} + E_Q + E_{st} + E_L \end{aligned} \tag{2}$$

To point out the product of the system, the terms of Eq. (1) could be grouped in the following way:

$$\begin{aligned} E_p = (E_{el} - E_{el}^i) + E_Q + E_{st} &= \\ = E_{el}^u + E_Q + E_{st} \end{aligned} \tag{3}$$

$$E_i = E_{com} + E_f^{com} \tag{4}$$

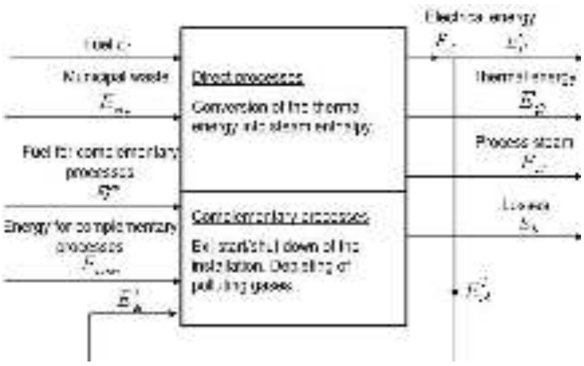

Fig. 1. *Schematic of the energy balance for the combined system, incinerator and steam turbine, for the energetic recovery of the municipal solid waste*

Accounting for equations (3) and (4), the energy balance equation (2) becomes:

$$E_f + E_{mw} + E_i = E_p + E_L \tag{5}$$

where Ep is the product of the system offered to external systems interested to buy it and E_L represents the losses with the energy thrown away into the environment for which, obviously, no money is earned.

The coefficient of performance of the system may be stated depending on the definition of the installation Product and Fuel.

If one wants to point out the net energy obtained by each product from the municipal waste, then Equation (5) becomes:

$$E_{mw} = (E_p - (E_f + E_i)) + E_L \tag{6}$$

where

$$E_{mw} = F_1 \tag{7}$$

and

$$E_p - (E_f + E_i) = P_1 \tag{8}$$

For this case, the coefficient of performance is:

$$COP_1 = \frac{P_1}{F_1} = \frac{E_p - (E_f + E_i)}{E_{mw}} = 1 - \frac{E_L}{E_{mw}} \tag{9}$$

By replacing Eq. (4) in Eq. (5), it gives:

$$E_f + E_{mw} + E_{com} + E_f^{com} = E_p + E_L \tag{10}$$

If one considers as Fuel the sum between the energy of the municipal waste (E_{mw}) then the energy of the conventional fuel is used in the auxiliary burners to maintain the prescribed temperature in the reactor (E_f).

$$F_2 = E_f + E_{mw} \tag{11}$$

Then by the identification of Eq. (10) with the equation (12) of the energy balance written with economic sense

$$F = P + L \tag{12}$$

the Product becomes:

$$P_2 = E_p - (E_{com} + E_f^{com}) = E_p - E_i \tag{13}$$

and as a consequence:

$$COP_2 = \frac{P_2}{F_2} = \frac{E_p - (E_{com} + E_f^{com})}{E_f + E_{mw}} = \\ = \frac{E_p - E_i}{E_f + E_{mw}} = 1 - \frac{E_L}{E_f + E_{mw}} \tag{14}$$

A last approach could be to consider as Fuel the entire energy utilized with direct or complementary effect for achieving the goal of the installation, namely to obtain electrical or thermal energy, or process steam.

$$F_3 = E_f + E_{mw} + E_i \tag{15}$$

as a consequence:

$$P_3 = E_p \tag{16}$$

and

$$COP_3 = \frac{P_3}{F_3} = \frac{E_p}{E_f + E_{mw} + E_i} = \\ 1 - \frac{E_L}{E_f + E_{mw} + E_i} \tag{17}$$

Observing that the energy loss due to its transfer into the environment is the same for all the approaches, it results that:

$$COP_1 \langle COP_2 \langle COP_3 \tag{18}$$

The second definition of the COP (COP2) is the closest to the definition given by the R1 criterion.

It must be pointed out that the R1 criterion as a coefficient of performance based on only the energetic balance cannot account for the internal losses or for the changes in the intensive parameters of the environment.

A better approach must use the exergy concept to account for both the quality and quantity of each kind of energy [4].

4. Conclusions

The coefficient of performance of any energetic system is the ratio between the Product of the installation and resources consumed with this aim, resources generically called Fuel.

The value of the coefficient of performance depends on the way one considers which part plays the role of the Product and Fuel in the system.

The proper estimation of the Fuel and Product opens the way to a more rapid procedure of optimization.

Criterion R1 of assessing the coefficient of performance of a system for the energetic recovery of the municipal waste represents just one point of view defined in the Waste Framework Directive (2008/98/EC) of the European Community.

The R1 criterion as a coefficient of performance is based only on the energetic balance and thatis why it cannot account for the internal losses or for the changes in the intensive parameters of the environment.

Correction must be added to the R1 criterion to account for the changes in the temperature of the environment.

References

[1]. Dobrovicescu A., Serban A., Prisecaru T., Apostol V., *Fuel and Product in the exergetic analysis of refrigeration systems*, The 24th IIR International Congress of Refrigeration, Improving Quality of Life, Preserving the Earth, Yokohama, Japan, 2015.

[2]. Wojciech Stanek, Editor, *Thermodynamics for Sustainable Management of Natural Resources*, Springer, 2017.

[3]. ***, *Guidelines of the interpretation of the R1 energy efficiency formula for incineration facilities dedicated to the processing of Municipal Solid Waste*, according to Annex II of Directive 2000/98/EC on Waste, 30/6/2011.

[4]. Dincer I., Rosen M. A., *Exergy Analysis of Heating, Refrigerating and Air Conditioning*, Elsevier, 2015.

THE ANNALS OF "DUNAREA DE JOS" UNIVERSITY OF GALATI
FASCICLE IX. METALLURGY AND MATERIALS SCIENCE
N°. 2 - 2017, ISSN 1453-083X

MANAGEMENT OF THE ENVIRONMENTAL RISKS IDENTIFIED IN AN ORGANIZATION

Tamara RADU, Bogdan LUNGU
"Dunarea de Jos" University of Galati, Romania
e-mail: tradu@ugal.ro

ABSTRACT

Response to risk is a process that is directly involved in risk management and is governed by the organization's security strategy, environmental characteristics and security mechanisms. The management identifies the options available to respond to the risk and analyzes the effects of these options on the likelihood and impact of a risk, in close connection with the availability for the risk and cost-benefit ratio, and then conceives and implements actions of response to risk. These steps are integral parts of risk management and contribute to bringing the level of risk within agreed tolerance limits. The paper presents the evaluation of risk management options and the way of environmental risk management decision making. The multi-criteria analysis of risk management options and the use of the precautionary principle are also presented.

KEYWORDS: risk management, options, decision making, multi-criteria analysis

1. Introduction

Environmental Risk Management (ERM), applied at the level of an organization with a significant environmental impact, ensures the organizational structure, responsibilities and efficient allocation of resources so as to manage all the environmental risks associated with the main activities and related activities performed by the organization. In this context, ERM has the role of ensuring a systematic review of the organization's exposure to environmental risks and developing well-targeted risk management programs based on this analysis. This systematic approach provides specific risk management benefits, including improved environmental performance, and responsible risk-response decisions with an effective cost / benefit ratio. A structured and systematic approach to risk management allows for adequate and properly targeted environmental protection measures while avoiding excessive or inadequate measures [1]. Developing structured and documented risk assessment and management was essentially determined by the recognition that the possibility of negative and undesired results of an activity cannot always be eliminated [2]. Therefore, there is a need for a way to evaluate the following issues:

- the severity and probability of these negative results;
- applying appropriate control measures with an effective cost-benefit ratio;
- acceptance or tolerance of remaining risk after the available control measures have been implemented.

The risk management is a particular type of management considering the main objective, namely making decisions to address risk or establishing a response to risk [2]. For this reason, the main steps are not only those proposed by the Deming cycle (planning, executing, verifying, improving), and all specialists in the field agree to go through the following specific steps for a good risk management:

- systematically applying policies, procedures and practices to identify hazards;
- analyzing the likelihood and consequences of these hazards;
- estimating (quantitative or qualitative) risk levels;
- assessing these risk levels based on relevant criteria and objectives;
- making decisions about the identified risks.

Response to risk is a process that is directly involved in the risk management and is governed by the organization's security strategy, with its environmental characteristics and security mechanisms. The top management or environmental manager identifies the options available to respond to the risk and analyzes the effects of these options on the likelihood and impact of a risk, in close connection with the availability of risk and the cost-benefit ratio, and then conceives and implements risk response actions. These steps are integral parts of risk management and contribute to bringing the level of risk within the agreed tolerance limits.

2. Evaluating the options for environmental risk management

In the process of assessing environmental risk management options, consideration should be given to the relationship between environmental protection and improvement so as to allow for sustainable and long-term economic growth [3].

Environmental security aims at achieving a better quality of life globally, both now and for future generations [4]. The overall objective is to make sure that the economic and environmental benefits are available to everyone. It has been recognized that achieving environmental security requires a collective partnership in the decision-making process for environmental protection. Therefore, environmental management strategies must take into account economic requirements, social needs and the ability of the environment to deal with spills, pollution and other disturbances, in order to support humankind and all other forms of life. Continued efforts are being made to develop specific methods for assessing environmental risks and choosing their management options such as they are, for instance those that support land-contamination risk management decisions [5-9].

Unacceptable environmental risks require appropriate management to bring them to a tolerable residual risk. The zero risk is a target usually not achievable or demonstrated. Evaluating options for reducing environmental risks is the process of identifying and selecting the most appropriate risk management strategy taking into account the constraints imposed by the decision-maker [10]. The systematic methods that can be used to compare and evaluate risk management options cannot be universally valid for all circumstances. There is usually the possibility of selecting or adapting an existing methodology, but there will always be cases that will require the development of new methodologies.

Risk mitigation opportunities can be found along the whole risk analysis approach. In identifying opportunities for risk reduction, the following aspects will be considered:

- eliminating the hazard (such as replacing a hazardous chemical with a non-hazardous one in the technological process);
- reducing potential consequences (e.g. reducing stocks of hazardous substances or increasing security measures);
- reducing frequency / probability (e.g. increasing the frequency of maintenance and repairs or monitoring or taking additional measures).

Risk reduction will concern both the whole system and:

- possible changes to some operational phases;
- changes to protective measures;
- essential changes, for example: relocation of installations, revision or replacement of technology, revision of the mode of transport.

It is important that risk management facilitates risk mitigation so as to adopt the management option that results in the lowest risk levels whenever they are affordable to an affordable price. Identifying risk mitigation opportunities will focus on their likely impact on risk levels. It is important to identify risk management options as a distinct preliminary step because inappropriate risk management strategies can lead to unnecessary efforts and expenses [10].

The available risk management options can be [4, 11-13]:

• eliminating the source of risk wherever possible;
• mitigating the effects of hazards by improving environmental management techniques or engineering systems;
• minimizing risk through new technologies, procedures or investments;
• exploiting the beneficial potential of risk by accepting new opportunities;
• accepting the risk of not intervening in new or existing situations;
• transferring the risk to a third party.

To select the appropriate risk management options, the potential positive and negative effects associated with each option will be assessed by analyzing at least the following factors [14]:

- technical factors: for example, the degree of research and development needed;
- economic factors: the cost of implementing the option;
- environmental security: the potential impact of options on health and sustainability of environmental resources, including impacts on existing habitats;
- social issues (social impact of risk) such as: potential costs or another loss to the community, jobs or housing prices, life expectancy, etc.;
- organizational capabilities - the ability to manage risks within the organization, other bodies, or the ability of the exposed society or groups.

Combining these elements allows for a systematic comparison of risk management options.

2.1. Economic considerations in choosing risk management options

Risk reduction can often be carried out at a low cost, and in some cases leads to substantial savings in operating or capital costs. Economic factors can have a significant influence on the decision-making process and may affect the acceptance of a given option. The best option will probably be the one that provides the greatest benefit achieved at the lowest cost. Benefits can come from reducing damage (avoiding damage or loss of property, material or cultural damage, damage to human health and environment). Benefits can also be achieved by reducing costs such as:

- social costs;
- regulatory costs and private costs;
- control costs, including construction and maintenance;
- the costs of remedying environmental damage.

Economic considerations should include both those benefits and costs that can be measured in money as well as those that cannot be measured as such, or for which accurate monetary assessments are not available. The latter must be evaluated physically and qualitatively. We need to make sure that the decision-making process pays same attention to all elements, without the non-valued ones being considered significant in relation to the elements that do not allow for such assessments. Applying a multi-criteria decision analysis can help to discern the benefits associated with various risk management options [4].

2.2. The role of criteria and objectives in choosing management options

Once the hazards have been identified and analyzed, the risk objectives or criteria set up at the beginning of the risk analysis can provide a rational and consistent basis for identifying risk mitigation options / options for assessing risk responses.

When risk analysis only aims at comparing cases and identifying options for the lowest risk, the analysis may be simple and no other criteria are required. When a risk analysis has the purpose of determining the level / rank of the risk and identifying the factors that can contribute most to risk, the need for criteria may be limited [15, 16]. For most analyses, however, the defined objectives and / or criteria are important. While the criteria are largely used towards the end of the analysis, identifying, selecting or developing relevant criteria should be made earlier than the end of the risk analysis and eventually improved over time. In this way, the criteria can be taken into account throughout the risk management process. This approach will help determine when a hazard can be removed from a more in-depth examination on the grounds that it has a low consequence or probability. Therefore, the results can be developed in an appropriate form for the assessment of management options according to specific criteria. In spite of this, economic considerations on benefits and cost effectiveness may become de facto criteria [17].

Even if criteria are important, it should be underlined that it is just as important that the risk analysis and management process do not become a criterion verification exercise, missing the main purpose of achieving a real improvement in safety and environmental protection.

3. Making decisions on environmental risk management

The best decisions on environmental risks require both the best scientific approach and the best decision-making processes. Decision-making will be based on information, knowledge, experience, concerns, research and understanding as well as support by the people who may be directly affected by them. Risk management involves all categories of staff, never being solely the responsibility of the top management or risk advisory organizations. Running the risk management process requires both commitment and decision-making power of the top management along with employee involvement, because the latter can first identify an incident, a potential hazard or an opportunity for improvement. In this approach, it is important for the decision maker to be fully informed about the objectives and the way to decide, especially when the choice is between the benefits of risk mitigation and the cost of introducing appropriate measures.

Appropriate decisions will be based on an effective and accurate assessment of alternative risk management options. A systematic assessment of the options will be a process of identifying and quantifying the costs and benefits of the measures to implement the environmental management. This process should include all possible options and implications, not just those that can be quantified. A framework for decision-making can include the following steps:

- well-defined identification of the target and the desired result;
- identifying the options for achieving the objective or the result sought;

- clarifying the decision criteria and the implications of applying an economic, social and environmental option;
- identifying the tools needed to implement options such as policy instruments, measures or economic regulations;
- identifying the impact of the options (in this respect it will be necessary to collect data from the stakeholders that will be affected by the potential measures);
- comparing the advantages and disadvantages of each option, including the compromise between quantified and qualitative data.

3.1. Multi-Criteria Analysis

The analysis of decision options, taking into account several criteria (also called multi-criteria analysis) such as economic, social and environmental criteria, is a complex approach, largely due to inherent compromises between these risk-affected areas.

Selecting an appropriate risk management strategy often involves additional criteria, such as environmental impact distribution or costs and benefits [18]. Decision-making research based on a multi-criteria analysis [19-21] has allowed for the development of practical ways to compare decision-making options when there are several criteria for assessing these options [22]. The main advantage of multi-criteria analysis is its ability to draw attention to areas of divergence between stakeholders and decision-makers. However, the need to reach a consensus with stakeholders on the main criteria in question may lead to limitations in the use of the method. Participants may initially be unprepared to give up their own opinions, but they may better understand an alternative option presented through a multicriterial analysis [23]. Multi-criteria decision analysis typically meets criteria and performance levels in the form of matrices to provide a basis for integrating risk levels and uncertainty. In this way, it is possible to carry out an assessment of alternative risk management options. Table 1 presents a multi-criteria analysis matrix of the decision on a risk management option.

The efficiency of the criteria according to the options being evaluated can be a two-step approach:

- First, how each option will affect the issue is presented in terms of positive and negative effects on the three main elements: environment, society and economy;
- Next, for the option considered optimal, the potential risks of applying that option (e.g. organizational capacity, complexity of implementation) will be considered.

For example, the decision matrix presented in Table 1 shows that decision 3 is the most effective in terms of risk reduction, but it is costly. Depending on the opinion of the decision-makers and the available budget, they can select decision 3 or a cheaper option, decision 2, which can still lead to an adequate level of risk reduction [22]. If the risk response becomes clear, the effectiveness of the action chosen by the risk management is then verified during the monitoring and risk assessment phases.

Table 1. *Multi-Criteria Analysis of Risk Management Options* [22]

Criterion	Decision 1	Decision 2	Decision 3
Economic	?	↑	↑
Environment	↑	↓	↓
Social	↑	↔	↓

↓ - decrease in risk level
↑ - increase in risk level;
↔ - insignificant impact on risk;
? - insufficient information or too many uncertainties to analyze the option impact.

3.2. Involvement of the interested parties/stakeholders and the public in decision-making

In some cases, it may be necessary to involve stakeholders and the public in the decision-making process on the choice of environmental risk management options. It is possible that those who were involved in defining the risk area or planning the risk assessment would like to be involved in the post-evaluation phases as well. This can be beneficial because good decisions are often based on the information, knowledge and concerns of stakeholders and the public and are understood and supported by people who may be directly affected by them (e.g. studies on genetically modified vegetables, designing a new food control system, granting license for land use, remediating a contaminated site). The involvement of stakeholders and the public in assessing risk management options can lead to positive results such as conflict resolution, social education [24], wider knowledge integration and community support [25]. In practice, the too late consultation of stakeholder decision-making [26] is no longer appropriate so as to actually influence the decision. The result may be public frustration, opposition to decisions made and requirements for more information, resulting in delays in decision-making. These difficulties have led to the adoption of analytical and deliberative decision-making processes in many countries that enable public involvement through analyses and debates on risk assessment and risk analysis (known as participatory risk assessment). Participatory risk assessment has been recognized as a valuable way to support public commitment.

In planning a risk assessment, public commitment should be ensured for:

• stakeholders and public opinion who can be considered in decision-making;

• the situation where there is, it is likely to be, or has been concern about the risk issue;

• support for stakeholders and the public for decision-making.

A participatory risk assessment process is joined by a bottom-up approach. This process aims at involving stakeholders and the public in: formulating the problem, assessing preferred management options, and proposing solutions to specific risk issues.

There may be several decision-makers (environmental authorities and agencies, NGOs, etc.) that need to be involved in the assessment of risk management options. In this case, it is important to clearly show to those involved the goals and limits of what can be achieved. For example, it may not be possible to change the land use decision, but it is possible to introduce conditions for construction and activities [1].

3.3. Relevance and use of the precautionary principle in decision-making

The precautionary principle may be invoked if a preliminary scientific assessment shows that there are reasonable grounds for concern that a particular activity could lead to harmful effects on the environment or on the health of plants, humans, animals or would be in conflict with the protection normally provided to them within the European Community. The precautionary principle states that "In order to protect the environment, a cautious approach is widely applied by states according to their capabilities. If there are threats of serious or irreversible damage, the lack of full scientific certainty will not be used as a reason for postponing measures to prevent environmental degradation "(Principle 15 of Agenda 21). If the precautionary principle is adopted, decision-makers establish:

- what action is necessary in view of the potential consequences if no action is taken;

- the uncertainties inherent in scientific evaluations;

- consultation of stakeholders on possible ways of risk management

The measures adopted must be proportionate to the level of risk and the desired level of security. They should provisional, pending the availability of more reliable scientific data. Research into the use of the precautionary principle [27] has already identified the following issues to be considered:

-admitting the lack of information;

- the need for long-term monitoring of the actual field conditions;

- taking into account the benefits;

- the use of local knowledge and expertise;

- avoiding lack of analysis and action to reduce potential injury when there are good reasons for concern.

4. Conclusions

The environmental risk management applied at an organization is intended to evaluate options for addressing the identified environmental risks and to make the best decisions to eliminate and minimize these risks.

Assessing the risk response options will be based on economic considerations, the best option will be the one that ensures the highest benefit achieved with the lowest cost.

The risk management involves all categories of staff and is never the sole responsibility of top management or risk advisory organizations.

Making appropriate decisions on ERM will be based on an effective and accurate assessment of alternative options.

The analysis of decision options, taking into account several criteria (also called multi-criteria analysis) such as economic, social and environmental ones, is an appropriate method of assessing decisions.

The involvement of stakeholders and the public in making decisions is important. This can be beneficial because good decisions are often based on the information, knowledge and concerns of stakeholders and the public.

The precautionary principle in management decision-making may be invoked if a preliminary scientific assessment shows there are reasonable grounds for concern that a particular activity of the organization could lead to harmful effects on the environment.

References

[1]. Dryden P., Beer T., Lambert I., *et al.*, *Environmental risk management*, Australia, 1999.

[2]. Tamara Radu, Maria Vlad, Marius Bodor, Gelu Movileanu, *Managementul riscului de mediu*, Galati University Press, Colectia Stiinte Ingineresti, 2015.

[3]. ***, *Defra's evidence investment strategy: 2010-2013 and beyond*, London, UK: Department for Environment, Food and Rural Affairs, (Defra 2010).

[4]. Gormley Áine, Pollard Simon, Sophie Rocks Edgar Black, *Guidelines for environmental risk assessment and management*, UK, 2011.

[5]. Tamara Radu, *Environmental risks assessment by qualitative and quantitative methods*, The Annals of “Dunarea de Jos”

University of Galati. Fascicle IX. Metallurgy and Materials Science, no. 3, p.43, 2016.

[6]. Radu Tamara, Balint Lucica, Istrate Gina Genoveva, Tudor Beatrice, *Environmental risk assessment by risk matrix method*, 17th International Multidisciplinary Scientific GeoConference SGEM 2017, Conference Proceedings, Albena, Bulgaria, June 28 - July 6, 2017.

[7]. ***, *A framework for assessing the sustainability of soil and groundwater remediation*, Contaminated land: applications in real environments (CLAIRE), 2010.

[8]. ***, *Network for industrially contaminated land in Europe*, (NICOLE), 2010.

[9]. ***, *Sustainable remediation forum*, 2010.

[10]. Treasury H. M., *The green book appraisal and evaluation in central government*, London, UK: The Stationary Office, 2003.

[11]. Ozunu A., Anghel C. I., *Evaluarea riscului tehnologic şi securitatea mediului*, Ed. Accent, Cluj-Napoca, 2007.

[12]. Pece St., Dascalescu A., *Metoda de evaluare a riscurilor de accidentare şi îmbolnăvire profesională la locurile de muncă*, PHARE – MMPS – ICSPM, 1998.

[13]. Mincă Gabriel, *Metode de evaluare şi prevenire a riscurilor profesionale bazate pe teoria fiablităţii sistemelor, suport de curs*, Universitatea Tehnică „Gheorghe Asachi" Iaşi, 2007.

[14]. ***, *Enterprise risk management: Practical implementation*, Aon Global Risk Consulting, Aon Corporation, 2007.

[15]. Tamara Radu, Anisoara Ciocan, Maria Vlad, Simion Ioan Balint, Viorel Dragan, *Environmental risk assessment in the galvanizing of steel sheets*, SGEM 2012, 12th International Multidisciplinary Scientific GeoConference Proceedings vol V, p. 391-397, 2012.

[16]. Tamara Radu, *Environmental Risk Assessment for Thermal Power Plants*, The Annals of "Dunarea de Jos" University of Galati. Fascicle IX, no. 4, p. 36-40, 2015.

[17]. ***, *EPE Rapport du groupe de travail, Les risques environnementaux vus par les entreprises, leurs banquiers et leurs assureurs*.

[18]. Steele K. S., Carmel Y., Cross J., Wilcox C., *Uses and misuses of multicriteria decision analysis (MCDA) in environmental decision making*, Risk analysis, 2009.

[19]. Tam C., Tong T., Chiu G., *Comparing non-structural fuzzy decision support system and analytical hierarchy process in decision-making for construction problems*, European Journal of Operational Research, 2006.

[20]. Chan J., Tong T., *Multi-criteria material selections and end-of-life product strategy: Grey relational analysis approach*, Materials and Design, 2007.

[21]. Higgins A., Hajkowicz S., Bui E., *A multi-objective model for environmental investment decision making*, Computers and Operations Research, 2008.

[22]. Kiker G. A., Bridges T. S., Varghese A., Seager T. P., Linkov I., *Application of multicriteria decision analysis in environmental decision making*, Integrated, Environmental Assessment and Management, 1, 2005.

[23]. Paruccini M., *Applying multiple criteria aid for decision to environmental management*, London, 1993.

[24]. Bull R., Petts J., Evans J., *Social learning from public engagement: dreaming the impossible?*, Journal of Environmental Planning and Management, 51, (5), p. 701-716, 2008.

[25]. Webler T., Tuler S., Krueger R., *What is a good public participation process? Five perspectives from the public*, Environmental Management, 27, p. 435-450, 2001.

[26]. Petts J., Brooks C., *Expert conceptualisations of the role of lay knowledge in environmental decision making: challenges for deliberative democracy*, Environment and Planning A, 2006.

[27]. ***, *Late lessons from early warnings: the precautionary principle 1896-2000*, European Environment Agency (EEA), Environmental issue report number 22, Luxembourg: Office for Official Publications of the European Communities, 2001.

THE ANNALS OF "DUNAREA DE JOS" UNIVERSITY OF GALATI
FASCICLE IX. METALLURGY AND MATERIALS SCIENCE
N°. 2 - 2017, ISSN 1453-083X

THE INFLUENCE OF MOISTURE ON THERMAL CONDUCTIVITY FOR BUILDING MATERIALS

Gelu COMAN, Krisztina UZUNEANU, Simona PARASCHIV
Thermal Systems and Environmental Engineering Department,
Faculty of Engineering, "Dunarea de Jos" University of Galati, Romania
e-mail: Gelu.Coman@ugal.ro, Krisztina.Uzuneanu@ugal.ro, Simona.Paraschiv@ugal.ro

ABSTRACT

The purpose of the study is to determine the influence of moisture on thermal conductivity for a range of building materials. A series of building materials and insulation materials have a porous, fibrous or granular structure, in which blanks are filled with air. If these areas are filled with moisture or water, the thermal conductivity of the material increases, and the insulation capacity decreases. The thermal conductivity of the analyzed materials was measured in accordance with ISO 8301 protocols.

KEYWORDS: water absorption; moisture; thermal conductivity

1. Introduction

The aim of the present study was to investigate the variation of thermal conductivity (k-value) with the moisture content of the autoclaved aerated concrete (AAC) blocks. We examined the thermal conductivity and the water absorption properties for three AAC specimens with different degrees of humidity. The k-value can be greatly reduced by the presence of moisture within the building materials.

The building materials are exposed to environmental influences (i.e. rain or humidity).

Due to diffusion processes as a consequence of gradients of the temperature or the humidity, the moisture content of the materials can increase. High temperatures at high moisture contents lead to a strong increase of the effective thermal conductivity because of pore diffusion. Building, structural and construction materials mostly have a porous structure.

The moisture content depends mainly on the pore ratio and the pore structure of the building materials. Materials with a high porosity can absorb and store more water than those of low porosity. Due to the pressure difference or to the capillarity, the moisture can spread into the entire volume [1].

A slight quantity of water can infiltrate into the material via the manufacturing process. Furthermore, moisture can be absorbed by the materials due to the outer weather conditions. Buildings under construction are particularly exposed to moisture stress. Precipitation has an impact on the building in different ways.

Heat transfer by conduction through the building envelope represents a major component of the total thermal load of buildings. Reducing conductive heat gain through the walls and roof by using effective thermal insulation could lead to a significant reduction in the thermal load and consequently a reduction of the overall electric energy consumption.

The thermal performance of the building envelope depends to a great extent on the thermal effectiveness of the building materials which is mainly determined by its k-value. The k-value is dependent on the material density, porosity, moisture content and average temperature difference. Published k-values and those reported by manufacturers are normally evaluated at standard laboratory conditions of temperature and humidity to allow for a comparative evaluation of the thermal performance. However, when placed in their locations in the building envelope, thermal insulation materials are exposed to different temperature and humidity levels depending on the prevailing climatic conditions, hence their actual thermal performance may substantially differ from the one predicted under standard laboratory conditions [3].

2. Experimental details

2.1. Materials

Autoclaved Aerated Concrete (AAC) is one of the most commonly used light-weight construction materials for contemporary buildings, especially due to its low density, unique thermal and breathing properties and high fire resistance. This material has, however, some disadvantages; for instance, its very high-water absorption capacity makes it susceptible to deteriorations due to water. For instance, it is often used together with incompatible plasters leading to problems at the interfaces, such as condensation, which leads to an increase in the water content of the wall section and some faults occur on the finishing. In the presence of moisture and/or water, the AAC blocks lose the thermal conductivity, and mechanical properties. In order to prevent such problems, it is essential to use waterproof and water vapor permeable plasters and/or finish coats in applications of AAC.

In order to achieve the objective of the study, three types of AAC were selected (Fig. 1). The technical specifications of the AAC samples given by manufacturer are presented in Table 1.

Table 1. *The technical specifications of the AAC samples*

Technical specifications	Sample 1	Sample 2	Sample 3
Dry bulk density kg/m^3	400	550	600
Thermal conductivity W/mK	0.092	0.13	0.15
The diffusion coefficient of water vapors	5/10	5/10	5/10
Dimensional stability mm/m	0.15	0.33	0.5
Reaction to fire - Euroclass	A1	A1	A1

Fig. 1. *The AAC samples*

2.2. Measurement apparatus

The thermal conductivity is determined by means of the heat flowmeter method. The concept of a heat flowmeter appears in ISO 8301: 1991 [7]. The specimen under test is placed between a hot plate and the heat flowmeter which is attached to a cold plate. The apparatus is surrounded by insulation.

The hot and cold plates are maintained at suitable constant temperatures, measured by surface thermocouples. A calibration constant for the individual apparatus is derived from testing a sample of the known constant thermal conductivity. By measuring the heat flowmeter output and the mean temperature of the test sample, the thermal conductivity is calculated using this calibration constant [9].

The Hilton B480 (Fig. 2) unit is based on the heat flowmeter method described. ISO 8301:1991 gives the range of sample sizes that can be used with this method of conductivity measurement. The Hilton B480 unit is capable of holding specimens of 300 X 300 mm and 75 mm thickness.

Fig. 2. *The Hilton B480 unit*

The Fourier equation (Eq. 1) provides the relationship between the parameters of the test samples and the sections.

$$q = \lambda \cdot A \cdot \frac{\Delta T}{\Delta x} \qquad (1)$$

where: q (W) and T (K) are the heat flow and temperature difference across the sample, respectively, A (m^2) is the area through which the heat flows, x (m) is the thickness and λ is the thermal conductivity of the samples.

The thermal conductivity λ is determined with equation [9]:

$$\lambda = \frac{x \cdot \left[\left(k_1 + \left(k_2 \cdot \bar{T}\right)\right) + \left(\left(k_3 + \left(k_4 \cdot \bar{T}\right)\right) \cdot HFM\right) + \left(\left(k_5 + \left(k_6 \cdot \bar{T}\right)\right) \cdot HFM^2\right)\right]}{\Delta T} \tag{2}$$

where: x (m) is the specimen thickness, k_1, k_2, k_3, k_4, k_5, k_6, are calibration constants, HFM (mV) heat flowmeter output, $\bar{T}$ (K) is the mean temperature and ΔT (K) is the temperature difference between the hot plate temperature and the cold plate temperature.

2.2. Wetting of the samples

The moisture w (%) content of the samples can be calculated using the following equation:

$$w = \left(\frac{m_w - m_d}{m_d}\right) \cdot 100 \tag{3}$$

where: m_d and m_w are the mass of the dried and the damped samples, respectively [1].

The thermal conductivity of a wetted material depends on the moisture content of the material.

For the building materials under the given conditions, the thermal conductivity values can be determined with equation:

$$\lambda_w = \lambda_d \cdot a \cdot t \cdot w \cdot e^{(-b \cdot w)} \tag{4}$$

where: λ_w and λ_d are the thermal conductivity of the wet sample and the dried sample, respectively, a and b are constants for the material that can be determined from the experiments, t is the wetting time and w is the moisture content [1].

The samples humidification was performed according to standard EN 1609 (1997): "Thermal insulating products for building applications. Determination of the short-term water absorption by partial immersion" [8].

3. Results of experiments

The measurement of thermal conductivity and of the amount of humidity/moisture absorbed was made over a four- hour period and a one- hour step. Then the sample humidification has continued for 24 hours to determine the w_p coefficient according to EN 1609 (1997) standard.

As a result, for all AAC samples, two different curves will be presented: the moisture content as a function of the wetting time, .and the thermal conductivity change as a function of the moisture content.

Figure 3 illustrates the variation in the moisture content of sample 1 depending on the humidification time. Considering that sample 1 is characterized by the lowest density, i.e. the highest absorption capacity, a significant increase in the amount of moisture absorbed in the first humidification hour is noticed. During the other three hours, an increase in humidity occurs but not so significant due to water filling of the sample pores in contact with water.

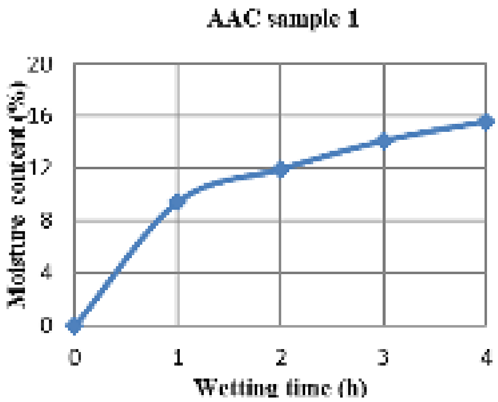

Fig. 3. *The moisture content as a function of the wetting time for sample 1*

Figure 4 shows the variation in thermal conductivity depending on the moisture content for sample 1. It can be noticed a significant increase in the thermal conductivity with the increase in moisture content, especially after the first humidification hour. For a humidity of approximately 15% the thermal conductivity increases four times.

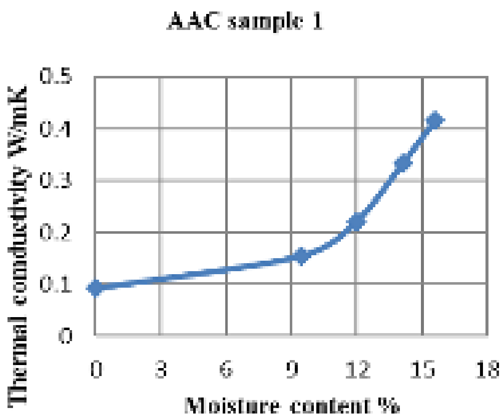

Fig. 4. *The variation of thermal conductivity vs. the moisture content for sample 1*

Figures 5 and 6 show the variation in the moisture content and thermal conductivity for sample 2. Unlike sample 1, there is a decrease in the amount

THE ANNALS OF "DUNAREA DE JOS" UNIVERSITY OF GALATI
FASCICLE IX. METALLURGY AND MATERIALS SCIENCE
N°. 2 - 2017, ISSN 1453-083X

of moisture absorbed due to the high density in sample 2. This is found in a lower variation in the thermal conductivity during the four hours of humidification.

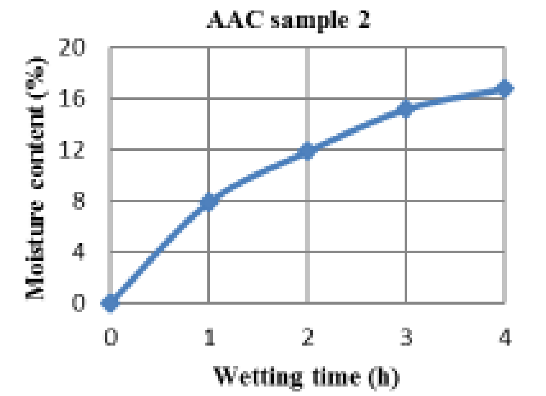

***Fig. 5.** The moisture content as a function of the wetting time for sample 2*

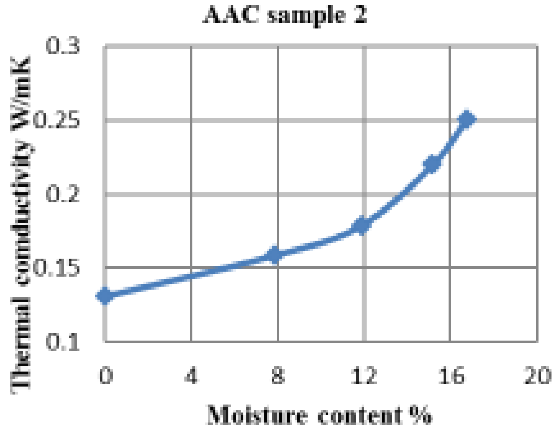

***Fig. 6.** The variation of thermal conductivity vs. the moisture content for sample 2*

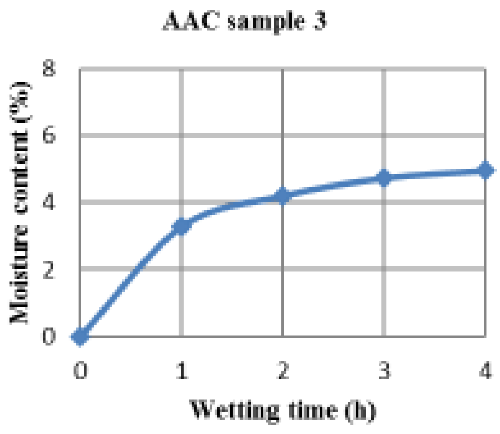

***Fig. 7.** The moisture content as a function of the wetting time for sample 3*

Compared to samples one and two, in the case of the third sample which is characterized by the highest density, a very low absorption capacity is observed during the four hours of humidification (Fig. 7). Although the dry sample 3 has the highest conductivity, it does not vary significantly due to the low absorbed moisture content (Fig. 8). The low absorption capacity for sample three is accounted for by the reduced number of pores in the material.

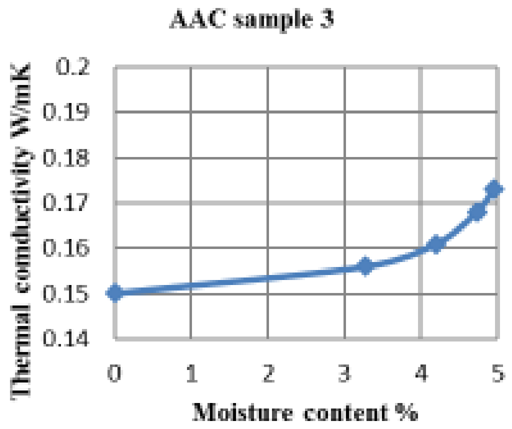

***Fig. 8.** The variation of thermal conductivity vs. the moisture content for sample 3*

4. Conclusions

The main purpose of the study was to experimentally determine the dependence between thermal conductivity and moisture content for three different types of AAC. In all three cases there was an increase in conductivity depending on the degree of humidification. Sample 1, although in dry state has the lowest conductivity, in the presence of moisture it loses its insulation capacity by increasing the conductivity coefficient.

With the increase in the density of the three samples, there is a decrease in the moisture absorption capacity but at the same time a decrease in conductivity. Therefore, when using AAC blocks, increased attention has to be paid to walls finishing and moisture exposure.

Generally, AAC constructions are externally covered by moisture resistant thermal insulation layers. At the same time, it is recommended that AAC blocks be stored in areas of low humidity before use.

The use of AAC blocks in the field of construction remains a very good solution both in terms of thermal insulation and mechanical strength.

References

[1]. Ferenc Szodrai, Ákos Lakatos, *Measurements of the thermal conductivities of some commonly used insulating materials after* *wetting*, Environmental Engineering and Management Journal, vol. 13, no. 11, p. 2881-2886, 2014.

[2]. Milo sJerman, Robert Cerny, *Effect of moisture content on heat and moisture transport and storage properties of thermal insulation materials*, Energy and Buildings, 53, p. 39-46, 2012.

[3]. Abdou A., Budaiwi I., *The variation of thermal conductivity of fibrous insulation materials under different levels of moisture content*, Construction and Building Materials, 43, p. 533-544, 2013.

[4]. Lakatos A., Kalmár F., *Analysis of water sorption and thermal conductivity of expanded polystyrene insulation materials*, Building Services Engineering Research and Technology, 34, p. 407-416, 2013.

[5]. Gawin D. J., Koniorczyk M., Wieckowska A., Kossecka E., *Effect of moisture on hygrothermal and energy performance of a building with cellular concrete walls in climatic conditions of Poland*, ASHRAE Transactions, 110, (Part II), p. 795-803, 2004.

[6]. Budaiwi I., Abdou A., Al-Homoud M., *Variation of thermal conductivity of insulation materials under different operating temperatures: impact on envelope-induced cooling load*, Journal of Architectural Engineering, 8, p. 125-132, 2002.

[7]. ***, *ISO 8301:1991. Thermal Insulation – Determination of Steady-State Thermal Resistance and Related Properties – Heat Flow Meter Apparatus*.

[8]. ***, *EN 1609:1997 Thermal insulating products for building applications - Determination of short term water absorption by partial immersion*.

[9]. ***, *Hilton 480-unit Instruction manual*.

THE ANNALS OF “DUNAREA DE JOS” UNIVERSITY OF GALATI
FASCICLE IX. METALLURGY AND MATERIALS SCIENCE
N°. 2 - 2017, ISSN 1453-083X

CALCULATION OF THE DEPOSITED LAYER THICKNESS THROUGH SIDE INJECTION OF POWDER USING CO_2 LASER

Simona BOICIUC, Petrică ALEXANDRU
“Dunarea de Jos” University of Galati
e-mail: simonaboiciuc@yahoo.com

ABSTRACT

The paper presents a simplified theoretical model for estimating the operating parameters of the laser deposition by injecting the powder into the metal bath. The study considered the influence of the powder particles on the transfer of energy from the laser beam to the surface of the substrate to be deposited. The following parameters were determined: the metal bath depth, the diameter of the metal bath, the mass of the powder deposited, the average temperature of the metal bath, the thickness of the deposited layer.

KEYWORDS: laser deposition by powder injection into the molten bath, determination of coat characteristics, influence of injected particles

1. Introduction

Laser deposition is used to improve the mechanical properties and corrosion resistance of layers at the surface of the materials.

As a superficial treatment of hardening, laser radiation processing aims at increasing the level of hardness of the surface layers, with a direct effect in terms of improving wear resistance. The specific characteristics of laser processing, namely ultra-fast heating speeds and variables in a wide range of values ($v > 10^3 \div 10^7$ $^oC \cdot s^{-1}$), high energy densities and a characteristic energy distribution into the beam, determine the particularities of the thermal transformations generated in the material being processed.

Laser deposition leads to a multi-zone structure: deposited layer, dilution layer where there is practically a surface alloying, a layer hardened in the solid phase, an annealed layer and finally the base material.

Laser processing, in hardening, alloying or deposition process, induces additional microstructural hardening mechanisms: over-saturation of the solid solution in carbon and alloying elements (martensitic hardening), increasing the degree of finishing of the structure and substructure respectively, a dispersion hardening or precipitation of carbides. The mechanism, the kinetics of these transformations, the morphology as well as the resulting properties are determined by the type of processing, the material under processing and the deposition material used.

Several models have been suggested for calculating the height of the laser deposited layer.

The theoretical model proposed in this paper involves a uniform distribution of the laser power and a one-dimensional heat flux inside the workpiece.

It is a simplified theoretical model used to estimate the dimensions of the molten layer and the deposited one, taking into account the parameters of the laser beam and the thermophysical characteristics of the support and the powder used. The influence of powder particles on the transfer of energy from the laser beam to the surface of the deposited substrate was considered using Mie's theory [1, 4, 5].

2. The theoretical model

For calculating the maximum height of the deposited layer, it was considered that this would be obtained for a maximum amount of thermal energy accumulated in the metal bath. However, the temperature at the bath surface should not exceed the boiling temperature of the support material.

Thus, the time dependence of conductive heat in the space under the irradiated surface is described by equation [1, 4, 5]:

$$\rho \cdot c \cdot \frac{\partial T}{\partial t} = k \cdot \frac{\partial^2 T}{\partial z^2} \quad (1)$$

Limit conditions will be:

$$k \cdot \frac{\partial T}{\partial z}(z=0) = (1-R) \cdot P/S$$

$$T(z=\infty) = T_0$$

where: ρ - material density; c – material specific heat; k – thermal conductivity; T – temperature; z – depth; P – laser power; R – reflexivity of the piece surface; D – diameter of the laser beam; v – laser motion speed; S – area of the laser irradiated surface.

The solution of this equation is (4):

$$T(z,t) = \frac{8 \cdot (1-R) \cdot P}{\pi \cdot k \cdot D^2} \cdot \sqrt{(a \cdot t)} \cdot e^{-\frac{z}{2 \cdot \sqrt{(a \cdot t)}}} \quad (2)$$

where: a – thermal diffusivity

The maximum local temperature achieved during the laser-material interaction for $t = D/v$ is:

$$T\left(z, t = \frac{D}{v}\right) = \frac{8 \cdot (1-R) \cdot P}{\pi \cdot k \cdot D^2} \cdot \sqrt{a \cdot D/v} \cdot e^{-\frac{z}{2 \cdot \sqrt{a \cdot D/v}}} \quad (3)$$

From eq. (3), the max. temperature of the irradiated surface may be written as:

$$T(z=0) = \frac{8 \cdot (1-R) \cdot P}{\pi \cdot k \cdot D^2} \cdot \sqrt{a \cdot D/v} \quad (4)$$

In laser deposition, however, where the powder is fed into the melt at the point where the beam strikes the substrate, the current power density that is distributed over the surface of the sample is lower than the apparent laser power by a factor that quantifies the transmission coefficient, φ. Thus:

$$P = \phi \cdot P_0 \quad (5)$$

where: P_0 – apparent power of the laser; φ - factor of attenuation

Thus, the temperature at the surface of the metal bath becomes:

$$T(z=0) = \frac{8 \cdot P_0 \cdot \phi \cdot (1-R) \cdot \sqrt{(a \cdot D/v)}}{\pi \cdot k \cdot D^2} \quad (6)$$

The temperature at the depth z inside the metal bath:

$$T(z) = \frac{8 \cdot (1-R) \cdot P_0 \cdot \varphi}{\pi \cdot k \cdot D^2} \cdot \sqrt{a \cdot D/v} \cdot e^{-\frac{z}{2 \cdot \sqrt{a \cdot D/v}}} \quad (7)$$

The attenuation coefficient of the laser beam intensity:

$$\varphi = \exp\left[-\frac{Q \cdot D}{m_p \cdot V_L \cdot v} \cdot D \cdot K \cdot \pi \cdot r_p^2\right] \quad (8)$$

But: $m_p = \rho_p \cdot V_p = \rho_p \cdot \frac{4}{3} \cdot \pi \cdot r_p^3$

K = 5, constant

$V_L = \frac{\pi \cdot D^2}{4} \cdot 5d$, laser operation volume

$Q = Q_0 \cdot \Gamma$, powder feed velocity

Γ - particle fraction contained in the metal bath

Then:

$$\varphi = \exp\left[-\frac{3 \cdot Q_0 \cdot \Gamma}{\pi \cdot r_p \cdot \rho_p \cdot v \cdot D}\right] \quad (9)$$

2.1. Calculation of the metal bath depth

In the case of laser deposition, it is desired to obtain a low- depth melt layer of approx. 0.3-0.5 mm. The model assumes that the ratio between the laser beam diameter and the maximum depth of the metal bath is $\frac{D}{z_m} \le 10$.

In eq. (7) make sure that at the depth $z = z_m$ the melting temperature T_m is reached.

$$T_m = \frac{8 \cdot (1-R) \cdot P_0 \cdot \varphi}{\pi \cdot k \cdot D^2} \cdot \sqrt{a \cdot D/v} \cdot e^{-\frac{z_m}{2 \cdot \sqrt{a \cdot D/v}}} \quad (10)$$

And at surface z = 0 temperature shall be acc. to the relation:

$$T(s) = \frac{8 \cdot P_0 \cdot \phi \cdot (1-R) \cdot \sqrt{(a \cdot D/v)}}{\pi \cdot k \cdot D^2} \quad (11)$$

Dividing T_m/T_s we get $T_m / T_s = e^{-\frac{z_m}{2 \cdot \sqrt{a \cdot D/v}}}$

By applying a logarithm to the expression, we reach the maximum depth of the metal bath:

$$z_m = 2 \cdot \sqrt{\frac{a \cdot D}{v} \cdot \ln \frac{T_s}{T_m}} \quad (12)$$

2.2. Calculation of the metal bath diameter

This is the actual diameter of the laser beam, d_e, as shown in Fig. 1. By setting the condition $T_s(z = 0) = T_m$ in equation (11):

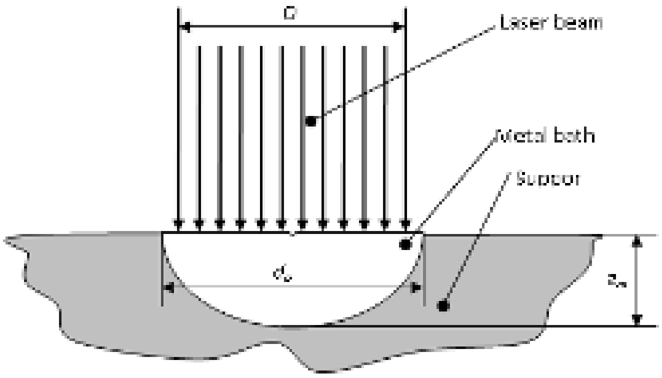

Fig. 1. *Image of the laser beam and the metal bath on the support*

$$T_m = \frac{8P_0\varphi(1-R)}{\pi k d_e^2}\sqrt{\frac{ad_e}{v}} \quad (13)$$

After squaring, we can obtain:

$$d_e = \sqrt[3]{\frac{64P_0^2\varphi^2(1-R)^2 a}{\pi^2 k^2 T_m^2 v}} \quad (14)$$

After squaring eq. (11):

$$T_s^2 = \frac{64P_0^2\varphi^2(1-R)^2 a}{\pi^2 k^2 D^3 v} \quad (15)$$

it is possible to obtain the sweep speed at which at temperature T_s, is obtained the melting temperature T_m and is reached at the bottom of the bath with z_m, depth:

$$v = \frac{64P_0^2\varphi^2(1-R)^2 a}{\pi^2 k^2 T_s^2 D^3} \quad (16)$$

Substituting this speed in eq. (14) the actual diameter of the laser beam can be determined:

$$d_e = D\sqrt[3]{\frac{T_s^2}{T_m^2}} \quad (17)$$

2.3. The approximation of the radius of the spherical calotte by which the shape of the metal bath is created on the support

From the rectangular triangle OAB, as seen in Fig. 2, it can be written: $OB^2 = OA^2 + AB^2$ (18), but,

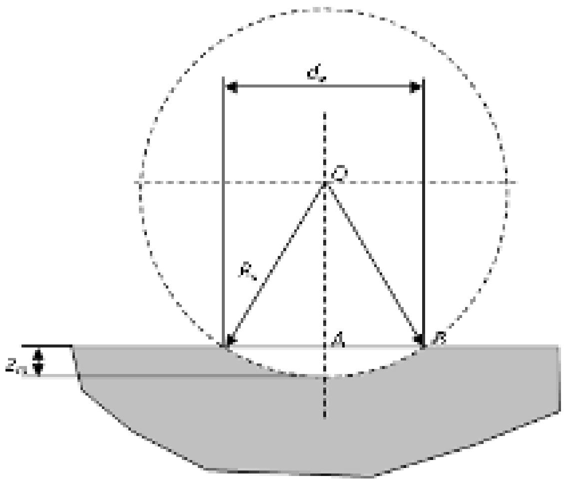

Fig. 2. *The characteristics (the radius Rs and the depth z_m) of the spherical calotte*

$$AB = \frac{d_e}{2}; OA = R_s - z_m; OB = R_s$$

After substituting them in the previous relation, we have:

$$R_s^2 = \left(R_s - z_m\right)^2 + \left(\frac{d_e}{2}\right)^2$$

2.4. Thermal balances, during the interaction time, $\left(t = \frac{d}{v}\right)$ in the metal bath injected with powder

Available energy in the metal bath to melt the injected powders:

$$\Delta E^s = m_b^s c_p^s \left[T_{mb}^s - T_{ma}^s\right] \tag{20}$$

- T_{ma}^s - apparent melting temperature of the support:

$$T_{ma}^s = T_m^s + \frac{L^s}{C_p^s}$$

- T_m^s - melting temperature of the support, [°C];
- L^s - latent melting heat of the support, [J/kg];
- C_p^s - specific calorific capacity of the support material, [J/(kg°C)];
- T_{mb}^s -average temperature of the metal bath formed on the support (no powder intake), [°C].

The energy required to melt the powder:

$$E^p = m^p \left[C_p^p \left(T_m^p - T^p\right) + L^p\right] \tag{21}$$

And finally, the radius of the spherical calotte is obtained to further approximate the metal bath:

$$R_s = \frac{1}{2}\left(z_m + \frac{d_e^2}{4z_m}\right) \tag{19}$$

- T_m^p - melting temperature of the powder [°C];
- T^p -powder temperature at the metal bath intake [°C];
- L^p - latent melting heat of the powder material [J/kg];
- m^p -mass of the molten powder [kg].

Equaling expressions (20) and (21):

$$m_b^s c_p^s \left[T_{mb}^s - T_{ma}^s\right] = m^p \left[C_p^p \left(T_m^p - T^p\right) + L^p\right]$$

the mass of the deposited powder can be calculated:

$$m^p = \frac{m_b^s c_p^s \left[T_{mb}^s - T_{ma}^s\right]}{\left[C_p^p \left(T_m^p - T^p\right) + L^p\right]}, \text{[kg]} \tag{22}$$

Since the maximum temperature of the metal bath and its maximum depth lie on the same perpendicular, to the surface of the bath and in its center, it results that there are conditions for melting a maximum amount of powder in this area. It can, therefore, be assumed that the deposited layer will be in the form of a spherical calotte, characterized by the values: h_m - the calotte height (laser deposition layer), z_m - maximum depth of the metal bath (molten layer) and de - the diameter of the base, as shown in Fig. 3.

2.5. Calculation of the average temperature of the metal bath - T_{mb}^s

Since the temperature distribution in the depth of the bath is given by equation (7), the temperature field is considered to consist of isotherms in the form of concentric spherical surfaces.

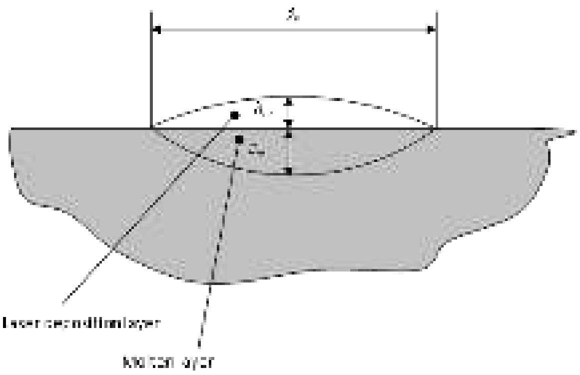

Fig. 3. *The characteristics of the laser deposition layer*

The volume of the metal bath will be divided into an infinite number of volume elements, as very thin sheets, of *dz* thickness and which practically fuse with the isotherms. The mean radius of each spherical sheet will be R (z) as shown in Fig. 4.

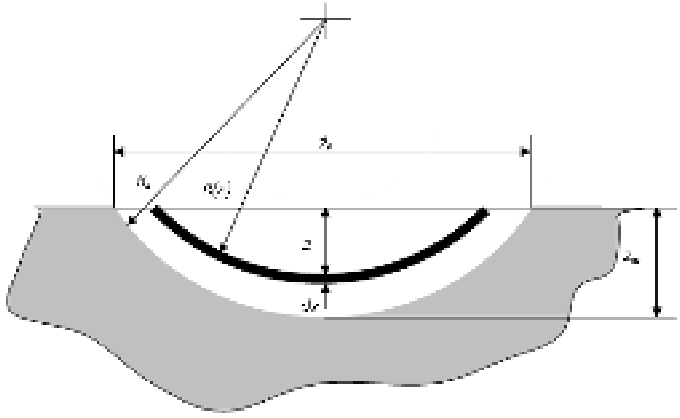

Fig. 4. *The characteristics of the volume of the metal bath*

Temperature of this volume element will be:

$$T(z) = \frac{8P_0\varphi(1-R)}{\pi k D^2}\sqrt{\frac{aD}{v}}\exp\left(-\frac{z}{2\sqrt{\frac{aD}{v}}}\right) \quad (23)$$

and the radius of the sphere considered for the middle of the element thickness:

$$R(z) = R_s - z_m + z$$

The volume of the volume element can be calculated by the expressions:

$$dV = 2\pi R(z) z dz$$

After replacing expression of *R(z)*:

$$dV = 2\pi\left[(R_s - z_m)z + z^2\right]dz$$

the average bath temperature shall be a weighted average of the type:

$$T_{mb}^s = \frac{1}{V_b}\int_0^{z_m} T(z)dV \quad (24)$$

where $V_b = \frac{\pi z_m^2}{3}(3R_s - z_m)$ is the volume of the metal bath calculated acc.to the formula of the spherical calotte; after substitution in relation (24) this becomes:

$$T_{mb}^s = \frac{3}{\pi z_m^2(3R_s - z_m)}\int_o^{z_m} T(z)2\pi\left[(R_s - z_m)z + z^2\right]dz$$

After replacing the expression of T (z) and solving the integral, the average temperature of the metal bath is obtained:

$$T_{mb} = \frac{96(R_s - z_m)(1-R)P_0\varphi}{z_m^2(3R_s - z_m)\pi k D^2}\sqrt{\frac{aD}{v}}\left\{2\sqrt{\frac{aD}{v}}\left(1+\sqrt{\frac{aD}{v}}\frac{4}{R_s - z_m}\right) - e^{-\frac{z_m}{2\sqrt{\frac{aD}{v}}}}\left[\left(z_m + 2\sqrt{\frac{aD}{v}}\right)\left(1+\frac{4}{R_s - z_m}\sqrt{\frac{aD}{v}}\right)+\frac{z_m^2}{R_s - z_m}\right]\right\} \quad (25)$$

2.6. The volume of the powder deposited on the support

To be calculated by the simple relation:

$$V^p = \frac{m^p}{\rho^p}$$

This volume will be distributed over the surface of the solidified metal bath of diameter d_e, in the form of a spherical calotte of height h_m.

2.7. Maximum thickness of the deposited layer

Taking into account the calculation of the volume of the spherical calotte, when the height and diameter of the base are known, the volume Vp can also be written as:

$$V^p = \frac{\pi h_m}{6}\left[h_m^2 - 3\left(\frac{d_e}{2}\right)^2\right]$$

which can be transformed into the 3rd degree equation with the unknown h_m:

$$\frac{\pi}{6}h_m^3 + \frac{\pi}{8}d_e^2 h_m - V^p = 0$$

The canonical form of the 3rd degree equation is: $y^3 + p \cdot y + q = 0$ which means:

$$h_m^3 + \frac{3}{4} \cdot d_e^2 \cdot h_m - \frac{6 \cdot V^P}{\pi} = 0$$

$$p = \frac{3}{4} \cdot d_e^2; \qquad q = -\frac{6 \cdot V^P}{\pi}$$

Note that the determinant of the equation:

$$\left(\frac{d_e^2}{4}\right)^3 + \left(\frac{3V^p}{\pi}\right)^2$$

is positive and then the equation shall have only one real solution which is exactly the maximum thickness of the deposited layer:

$$h_m = \sqrt[3]{\frac{3V^p}{\pi} + \sqrt{\left(\frac{d_e^2}{4}\right)^3 + \left(\frac{3V^p}{\pi}\right)^2}} + \sqrt[3]{\frac{3V^p}{\pi} - \sqrt{\left(\frac{d_e^2}{4}\right)^3 + \left(\frac{3V^p}{\pi}\right)^2}} \tag{26}$$

3. Conclusions

The model proposed in this paper is a simplified theoretical model used to estimate the dimensions of the molten layer and the deposited one, taking into account the parameters of the laser beam and the thermophysical characteristics of the support and the powder used.

The model assumes uniform distribution of the laser power across the laser beam and one – dimensional heat flow into the workpiece.

The influence of the powder particles on the transfer of energy from the laser beam to the surface of the substrate to be deposited was considered.

The following parameters were determined: the metal bath depth, the diameter of the metal bath, the mass of the powder deposited, the average temperature of the metal bath, the thickness of the deposited layer.

References

[1]. Medres B., Bamberger M., Shepeleva L., *Mathematical modeling for laser treatment processes*, Surface Technologies Ltd. Israel.

[2]. Medres B., *Thermal and plasma phenomena in laser hardening and alloying of toolsteels*, Moscow, IMET, p. 284, 1989.

[3]. Bokren C., Huffman D., *Absorption and scattering of light by small particles*, John Wiley, p. 246, 1983.

[4]. Schneider M. F., *Laser cladding with powder*, Ph. D. Thesis University of Twente, Enschede, Olanda, 1998.

[5]. Vollertsen F., Partes K., Meijer J., *State of the art of Laser Hardening and Cladding*, Proceedings of the Third International WLT – Conference on Lasers in Manufacturing 2005, Munich, june 2005.

[6]. Levcovici S., Levcovici D. T., Gheorghieş C., Boiciuc S., *Laser Cladding of Ni-Cr-B-Fe-Al Alloy on a Steel Support*, The International Thermal Spray Conference and Exposition (ITSC), p. 1339-1344, Seattle, USA, May 15th-17th 2006.

[7]. Levcovici D. T., Boiciuc R., Levcovici S. M., Gheorhieş C., *Laser cladding of M2 steel on a steel substrate*, The International Thermal Spray Conference and Exposition (ITSC), p. 1333-1338, Seattle, USA, May 15th-17th 2006.

THE ANNALS OF "DUNAREA DE JOS" UNIVERSITY OF GALATI
FASCICLE IX. METALLURGY AND MATERIALS SCIENCE
N°. 2 - 2017, ISSN 1453-083X

EXPERIMENTAL RESEARCH ON INCREASING THE DURABILITY OF CAST ATCSi 5 Cu 1 ALLOYS FOR SEA SHIPS THROUGH HEAT TREATMENT

Adrian DIMA[1], Iulia-Margareta DIMA[2]
[1]"Gh. Asachi" Tehnical University of Iasi
[2]Scoala Gimnazială "I. Simionescu" Iași
e-mail: adima@tuiasi.ro

ABSTRACT

This paper presents an experimental research study on the utilization of complex heat treating on aluminum alloys in order to increase their durability. The practical usage of the studied aluminum alloys (more specifically, silumin type alloys) is envisaged to be in marine industry, where fatigue is very important, especially in corrosive medium. The applied complex heat treating is of tremendous importance and the results can be very good.

Durability means a combination of different characteristics that determine the time period in which a cast part can be used in safe conditions. For a seagoing ship condition, the durability of ATCSi 5 Cu 1 cast parts depends especially on mechanical resistance and corrosive resistance in marine water.

The present work investigates the possibilities offered by different heat-treating techniques in order to increase the overall durability of the seagoing ship parts by increasing the mechanical resistance and reducing the corrosion in sea water.

Thus, we conceived an original methodology of experimental research comprising of an optimum combination of adequate heat treating, static and dynamic tests as well as corrosion tests under pressure in conditions similar to sea water.

KEYWORDS: aluminum alloys, heat treating, durability, intercrystalline corrosion

1. Introduction

Applying thermal treatments to cast aluminum alloys is carried out in order to increase the mechanical strength characteristics or to increase certain physicochemical properties, ideally together. These types of thermal treatments are "quenching solutions" followed by artificial aging. Solution quenching leads to solubilization, dissolution of precipitated phases from the structure to a rigorously determined temperature followed by fast cooling in order to retain the dissolved atoms in the solution and to maintain a certain number of vacant sites in the network in order to increase possibilities of diffusion at low temperatures, thereby obtaining a solid supersaturated solution at room temperature, which is the optimal condition for hardening by precipitation. At the same time, corrosion resistance can be improved by slowing down using a rigorously controlled cooling jacket. For these reasons, it results that the choice of temperature-time cycles for the thermal treatment of artificial aging should be done very carefully depending on the desired purpose 1).

The basic requirements for an aluminum alloy to be thermally treated by solution hardening and artificial aging [1, 2, 4] are those that must allow for solid phase transformations in the equilibrium diagram. These alloys can withstand an order-disordered-hardening reaction.

2. Materials and methods

The ATCSi 5 Cu 1 alloy is a complex siluminous alloy from which pots used in the naval industry can be poured, an alloy that allows the structural hardening phenomenon by suitable heat treatments because magnesium forms intermetallic phases with silicon or aluminum, phases having variable solubility in the solid state of the Al_2Cu type.

The research methodology essentially presents the following steps:

- determination of chemical composition (Table 1);
- making Amsler study specimens (Fig. 1);
- experimentation of various cycles of complex thermal treatments, cycles covering STAS 201 / 2-80 indications.

Table 1. *Determination of chemical composition*

Type of alloy		Chemical composition					Impurity	%	
	Cu	Si	Mg	Mn	Al	Fe	Zn	Pb	Ni
ATC Si 5 Cu 1									
STAS 201/2- 80	1-1.5	5- 6	0.3-0.6	0.2-0.5	rest	0.8	0.5	0.2	0.3
charge exp.	1.15	5.4	0.32	0.25	rest	0.55	0.2	-	-

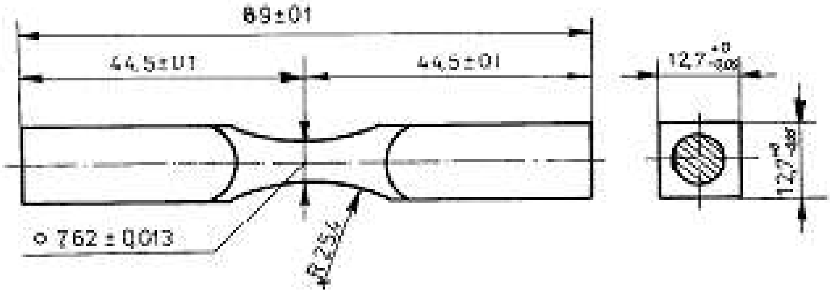

Fig. 1. *Amsler specimens*

Fig. 2. *Oval furnace of thermal treatments*

The ATC Si 10 Mg alloy is widely used in the naval industry. The alloy has the potential for structural hardening through the appropriate heat treatments, since magnesium forms intermetallic phases with silicon or aluminum, phases having a solid state variable solubility type Al2Cu.

The research methodology presents the following steps:

- determination of chemical composition (Table 1);
- realization of Amsler study specimens (Fig. 1);
- experimentation of various treatment cycles thermal complexes, indicating cycles data by STAS 201/2 -80 (SREN 1706/2000), (Table 2);
- determination and analysis of the main static and dynamic mechanical properties;
- determination of fatigue strength reduction due to stress corrosion effects (durability to breakage at constant effort).

The research methodology approached made possible the experimental determination of the correctness of the theoretical hypothesis of correlation between mechanical characteristics and susceptibility to stress corrosion developed by Thomas and Nutting, respectively Speidel and Engell [1-4].

Thermal treatments were carried out in oval furnaces of heat treatment (Fig. 2) according to STAS 201/2 -80 (SREN 1706/2000), (Table 2).

The research methodology approached made possible the experimental determination of the rightness of the theoretical assumptions of correlation between mechanical characteristics and susceptibility to stress corrosion developed by Thomas and Nutting [1, 3, 4] respectively Speidel and Engell.

Table 2. *Thermal treatments in oval furnaces*

Type of alloy		Heat experienced treatments				
		Burning			Aging	
	Heating temp. °C	Maintaining time	Cooling med.	Heating temp. °C	Maintaining time	Cooling med.
ATC Si 5 Cu 1	520 °C	6 h	water at 90°C	140, 160, 180	4-12	air

Thermal treatments have been carried out in heat-treated oval heat treatment furnaces (Fig. 2), which provide excellent sealing of the working space as well as different heating speeds due to the highly efficient controller from Euroline Inc.

Tensile strength tests were performed on the Amsler 40ZD 1094-1973 traction test machine.

Tests for fatigue resistance and stress corrosion resistance were performed on a Amsler NPL 434 type machine, a load-carrying machine with a centrifugal care mechanism providing 1500 cycles per minute.

For the stress corrosion study, the Amsler NPL 434 construction bolts were modified to overlap the mechanical stress of the corrosive coating agent (3.5% aqueous NaCl) on similar seawater.

For the mechanical and stress test for stress corrosion or for each thermal treatment cycle, 5 specimens (in the diagrams presented in the paper we use the average obtained values)

3. Experimental results

The tensile strength (R) obtained from the experimental thermal treatment cycles for the ATC Si 5 Cu 1 alloy shows a maximum increase over the casting state of the alloy of 24.80-daN / mm^2 for the thermal treatment cycle containing an artificial aging at 160 °C for 7 hours (Fig. 3). The average tensile strength obtained from the heat treatment cycles applied (Fig. 3) is superior to the minimum mean value of STAS 20l / 2-80 (R = 22 daN / mm), for thermal treatment cycles that only contain an artificial aging at 160 °C with a residence time of 4-10 hours.

Following the study of the value tables and the graphs of the average variation curves of the static mechanical characteristics, it is found that a complex thermal treatment consisting of hardening and artificial aging at 160 °C with a holding time of 7-8 hours leads to the optimal mechanical properties obtained after treatment for the ATCSi 5 Cu 1 alloy.

Corrosion-resistance durability curves (in 3.5% NaCl solution overlapping a mechanical stress of 14 daN / mm^2) until the experimentally determined test specimens are broken down as:

lg N = f (t), in which:

N - stress cycles up to breakage;

t - the holding time at the constant temperature of artificial aging, hours.

Aluminum alloys that are suitable for plastic deformation are much more researched in terms of physical-mechanical and structural properties due to their predominant use in car body construction.

Casting alloys, of which complex copper, or magnesium alloys, are increasingly being used to cast parts that are required at varying loads, which leads to the need to study their fatigue behavior.

The approach of the experimental researches carried out to determine the fatigue behavior of the alloy studied was also determined in order to study the stress corrosion behavior of the ATC Si Cu Cu alloy in casting or thermally treated after different thermal treatment cycles in the research.

The experimental research methodology of the variation of fatigue strength and stress corrosion, depending on the thermal treatments applied [1], adopted in the frame of the paper consists of:

1. Achievement of Amsler-type specimens (Fig. 1) needed to study the fatigue resistance of stress corrosion and durability to stress corrosion at the mechanical stress of cyclic bending constant;

2. Determination of fatigue resistance Wõhler curves of the studied alloys as well as tempered and artificially aged at 160 °C for 7 hours to study the influence of thermal treatments on the resistance to fatigue.

In the experimental research studies on the variation curves were plotted:

$$\lg 1 = f (1\text{g } N)$$

where: lg 1 is the bending fatigue resistance for the symmetrical alternating cycle, daN / mm^2.

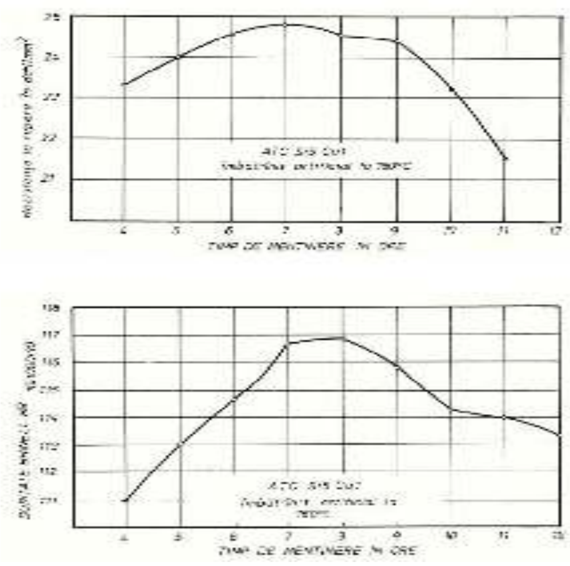

Fig. 3. Static mechanical tests

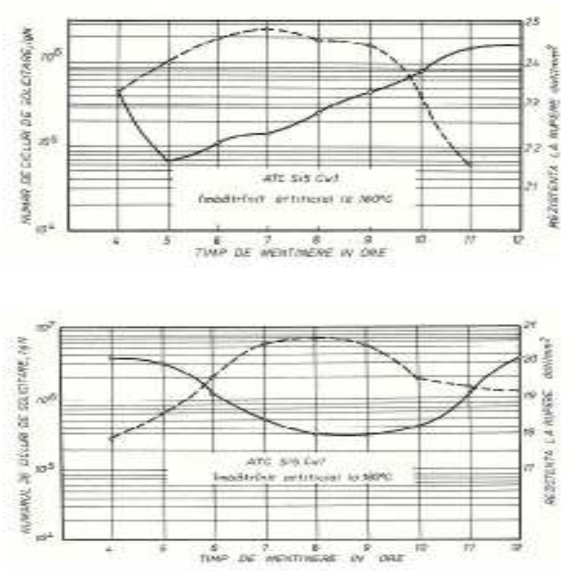

Fig. 4. Dynamic mechanical tests

For the determination of Wöhler fatigue curves for cyclic variable and alternating symmetrical bending variables, the classical working methodology was used, taking a number of 14-16 samples for each trace curve.

For the studied alloys, for the determination of fatigue resistance, the number of cycles of stress at 10^8 cycles was limited. Similarly, we also proceeded to determine the resistance to stress corrosion.

In the experiments, we have drawn Wöhler type charts, in semilogarithmic coordinates, for the cast alloy and aged at 160 °C (Fig. 4). At the same time, with the same methodology, we traced the Wöhler stress corrosion resistance curves for the cast alloy and artificially aged at 160 °C and 180 °C (Fig. 4).

These parallel experimental tests were necessary to highlight the influence of corrosive agent overlapping (seawater, 3.5% NaCl solution) the symmetrical bending cycle on the fatigue strength of the alloy, studied in the mold and artificially aged at 160 °C, after pre-setting at 520 °C for 6 hours.

From the study of Wöhler fatigue curves, it can be noticed that in the case of stress corrosion, the fatigue strength limit decreases from 4 daN / mm² to 3.2 daN / mm². For the ATCSi 5 Cast 1 alloy it is noted that by applying complex heat treatment cycles containing aging at 160 °C, cycles that lead to optimal mechanical properties, the fatigue strength increases from 4 daN / mm to 10 daN / mm. Applying stress corrosion to heat-treated alloys reduces fatigue strength, which is still superior to 2 daN / mm² for the studied alloy. It should be noted that the experiments carried out on the live corrosion confirmed the non-asymptomatic aspect of the aliasing of the variation curves at 10^8 load cycles.

For tracing the durability curves to stress corrosion at constant mechanical stress, depending on the time, the heat treatment is maintained for artificial aging, or using sets of 18 specimens, two for each holding time. The specimens used were checked for roughness and ovality.

From the study of the mean points of durability diagram for the ATC Si 5 Cu 1 alloy, it can be observed that the minimum lifetime of corrosion resistance is at a maintenance time of about 6 hours. For this value of the holding time, the maximum durability is represented by the artificially aged specimens (3.3 x ≦ 10〗 ^ 8 stress cycles) at 160 °C (Figure 4).

The variation curves of the corrosion resistance of the alloy studied will be used in the work in correlation with experimentally determined physico-mechanical characteristics.

In conclusion, the experimental determinations have highlighted the fact that the application of complex thermal treatment cycles of structural hardening totally leads to the increase of the fatigue resistance and of the resistance to the corrosion under tension of the studied alloy.

Thermal treatments for structural hardening are therefore a very effective method of reducing the effects of stress corrosion on foundry aluminum alloys while increasing the static and dynamic characteristics of resistance.

From the diagrams of the average values obtained for the ATC Si Cu 1 alloy (Fig. 4) diagram drawn for distinct temperatures of thermal treatment of artificial aging, the following main aspects are important:

In the case of the ATC Si 5 Cu 1 alloy (Fig. 4), the Speidel and Engell hypothesis is verified, the maximum mechanical characteristics being different from the minimum resistance to corrosion under voltage [3, 4]. Only for the artificially aged ATC Sil5 Cu 1 alloy 180 °C, we can consider valid (for experimental mean values) Thomas' hypothesis, too.

From the point of view of the temperature of thermal treatment of artificial aging, it is noted that a thermal treatment of artificial aging at 160 °C (Fig. 3, Fig. 4) leads to the highest values, both in terms of the resistance to traction and resistance to corrosion under voltage.

In conclusion, a complex heat treatment solution, followed by artificial aging (Fig. 4) at 160 °C for 10 hours, simultaneously leads to the maximum tensile strength correlated with a high resistance to corrosion under tension.

4. Conclusions

Based on the research work carried out, the following aspects can be highlighted:

1. The research carried out completes the knowledge of the possibilities of applying thermal treatment cycles to complex cast aluminum alloys;

2. In the field of theoretical and experimental foundation of the influence of the duration of maintenance on the thermal treatment of artificial aging on susceptibility to the corrosion under voltage, the following important conclusions are reached:

- the application of thermal treatments of structural hardening leads to the increase of the mechanical characteristics and the resistance to the corrosion under voltage;
- the theoretical hypothesis elaborated by Speidel and Engell is confirmed in the case of "Corrosion Fatigue" stress corrosion, too;
- resistance to corrosion under stress is minimal when the alloys exhibit a non-homogeneous supersaturated solid structure and begins to increase with the occurrence of separation processes of the precipitation equilibrium;

3. A contribution is the accomplishment, by constructive modifications, of the Amsler NPL-434 type fatigue test machine, to a corrosion-fatigue corrosion test machine;

4. The experimental results obtained confirm the validity of the methods for determining the maintenance time for artificial aging, which gives high resistance to corrosion under voltage;

5. Experimental temperature and maintenance time were determined for heat treatment of artificial aging to provide the physical and mechanical properties or the corrosion resistance desired;

6. The method of research used in the research on the effects of thermal treatments applied to cast aluminum alloys is an original contribution, as it also allows to study the intensity of the main physico-mechanical and structural characteristics;

7. Research on the possibilities of decreasing the effects of stress corrosion by application of thermal treatment cycles has highlighted that this method of reducing corrosion under tension is particularly advantageous since at the same time it is possible to obtain optimal physico-mechanical properties.

The prospects for further research are evident, as similar research can be done on other types of non-ferrous alloys.

References

[1]. Dima Margareta Iulia, *Researchers regarding the improvement of physical and mechanical properties of cast aluminum alloys using heat treatment*, University of Brasov, Ph.D Thesis, 2010.

[2]. Dima Adrian, Dima Margareta Iulia, Minea Alina, *Studies Concerning the Enhancing of the Mechanical Characteristics of the Aluminium Cast Alloys by Heat Treatments*, Buletinul IP Iaşi, tomul LII (LVI), Fasc.1 Secţia SIM, Iaşi, p. 117-120, 2006.

[3]. Dima Adrian, Minea Alina, Dima Margareta Iulia, *Researches for the Determination of the ATC Si 10Mg Alloy Fatigue Life, Function of Different Applied Thermal Treatment Cycles*, The Annals of "Dunarea de Jos" University of Galati Fascicle IX Metallurgy and Materials Science, p 16-19, nr. 1, 2005.

[4]. Engell H. V., Speidel M. O., *Werkstoffe und Korrosion*, Bd. 81, nr. 45, p. 79-95, Bd. 81, nr. 5, p. 77-83, 118, 120, 122, 1962.

THE ANNALS OF "DUNAREA DE JOS" UNIVERSITY OF GALATI
FASCICLE IX. METALLURGY AND MATERIALS SCIENCE
N°. 2 - 2017, ISSN 1453-083X

CONTRIBUTIONS TO INCREASING THE QUALITY OF URBAN LIFE THROUGH THE USE OF AN INTELLIGENT ROAD TRAFFIC MANAGEMENT SYSTEM

**Bogdan Gabriel CARP[1,2], Mihai GINGĂRAŞU[2*],
Narcisa Cela PÎNZARIU[3], Serghei PALAŞ[4], Daniela Laura BURUIANĂ[2]**

[1] A. I. Cuza Police Academy, Bucharest, Romania
[2] Faculty of Engineering, "Dunarea de Jos" University of Galati, Romania
[3] University of Sheffield, England
[4] Technical University of Moldova
e-mail: mihaigingarasu@yahoo.com

ABSTRACT

Traffic congestion is a phenomenon which occurs when road traffic is disturbed. In Galati city, traffic congestion increases rapidly due to an increase in the number of vehicles on the road. This work is an attempt to analyze the effects of traffic congestion by applying the waiting theory. Traffic congestion is frequent during the day, and the locals accept it as a daily routine. Urbanization in developing countries indicates that more people live in cities than before. The trend of urbanization, the population growth and the increasing number of registered vehicles put pressure on traffic and make life in the urban area more difficult. General data congestion and congestion management are the mitigation measures proposed but they are labor intensive and a heavy investment would be needed. Therefore, in order to find feasible measures, latest technologies such as GIS and GPS help analyze the live traffic situation and suggest cost effective measures to alleviate congestion. A previous attempt was effective in data collection, data analysis and display of results [1, 2]. A Geographic Information System (GIS) is a computer-based mapping tool that geographically analyses events and phenomena occurring on Earth. GIS technology integrates common database operations such as query and statistical analysis with unique viewing and the benefits of geographic analysis provided by maps [2]. In Galati, the GIS system is still not applicable because it has not been purchased by the competent authorities. In Romania, the GIS system is partially implemented. The traffic congestion has begun to be solved globally through GPS positioning technology with vehicle data collection, transport and operation. Using GPS Vehicle will provide direct and objective data on the behavior and status of the trip and the transport system that influences this behavior [3].

KEYWORDS: GPS, GIS, vehicle, traffic congestion, urban life

1. Introduction

Nowadays, there are a number of challenges lying ahead of the transport system. The idea of a Single European Transport Area, promoted by White Paper for Transport 2011, sets the goals to be achieved by 2050. The transportation has to become more competitive and resource efficient within this time frame. The goals for urban transport, in this respect, are to promote the use of cleaner cars and cleaner fuels. The need is also to reduce the number of fatalities and incidents. Yet another challenge is that the amount of traffic in Europe's urban areas has been increasing rapidly during last decades. The task of people involved in urban traffic management is to best allocate the scarce resources of road and kerbside space to potentially competing transport modes, within a network that has finite capacity. A more accessible public transport system has to be prioritized in traffic management.

2. Applications in traffic congestion management

The intelligent system for traffic management implemented in England made an impact in UE legislation by contributing mainly to an increase in the quality of urban life. England, even though they leave UE, is looking for a continuous improvement of the intelligent system of traffic especially because the safety of the population is the most important. The safety of people is achieved by decreasing the number of accidents and by increasing the quality of urban life through controlling and considerable reduction of pollutant emissions in areas with high traffic.

Traffic congestion occurs when a volume of traffic or modal split generates demand for space greater than the available street capacity; this point is commonly termed saturation. A 2011 study in *The American Economic Review* indicates that there may be a fundamental law of road congestion. The researchers, from the University of Toronto and the London School of Economics, analyzed data from the U.S. Highway Performance and Monitoring System for 1983, 1993 and 2003, as well as information on population, employment, geography, transit, and political factors. They determined that the number of vehicle-kilometers traveled (VKT) increases in direct proportion to the available lane-kilometers of roadways. The implication is that building new roads and widening existing ones only result in additional traffic that continues to rise until peak congestion returns to the previous level [4, 5].

2.1. Decision-makers in policy-making

The role of intelligent transport systems is generated by problems caused by traffic congestion and the development of new information technologies for real-time simulation, control and communication networks, offering the ability to address issues such as managing urban traffic in an innovative environment. Traffic congestion has increased as a result of increased traffic motor vehicles, population growth and changes in population density. Increased urbanization has led to many large cities experiencing high traffic levels in the peak hours, traditionally between 07.00-10.00 and 16.00-19.00. The result is that the road network in many urban areas in Europe operates at or near capacity during several days. The problem of traffic congestion is an increasingly pressing issue and because of the harmful effect it has, there is an increased need to mitigate its consequences.

Congestion reduces the efficiency of transport infrastructure and has negative impacts on travel time and reliability, increases fuel consumption and air pollution. Congestion also has a particularly negative effect on the economy distribution services.

3. Intelligent transport systems to reduce congestion in urban traffic

Proposed intelligent transport systems allow to reduce significantly the idle time in traffic congestions and to increase movement speed of traffic participants, to reduce electrical energy and fuel consumption. Such a solution allows to save up to 26% of electrical energy of the total consumption by city transport, as well to reduce idle time for electric transport at crossroads up to 13% and increase traffic speed up to 28% [6].

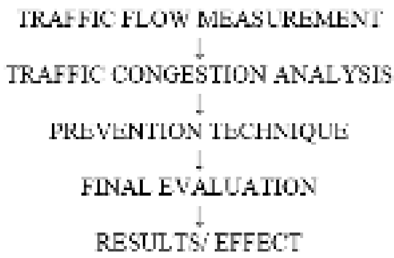

Fig. 1. *Steps for Preventing Traffic Congestion*

Galati City, one of the most important economic centers in Romania, is under a continuous pressure determined by the increasing road traffic. The system bought responded to the identified needs by the council of the city through the implementation of a complex program to manage the traffic. This included sub-systems of traffic lights, road signaling, communications, urban video surveillance, automatic identification of vehicles' registration numbers, defects management. All the systems will be coordinated in a performant center of control [7].

In Galati county, the intelligent system to manage the traffic on city roads is relatively new, being implemented in august 2016. The purpose of implementing this intelligent system is to fluidize the traffic, to increase the safety of the traffic participant, to reduce the number of accident and road blockages, but also to reduce pollution.

The implemented system is in accordance with the European regulations and allows for the identification in real time of traffic situation, communication between crossroads, modification of traffic lights time considering the number of vehicles. This generates a fluency of vehicles in all 35big crossroads in the city. Also, 26 crosswalks contain synchronized and adapted lights, with an activation system by button which can be pressed by pedestrians. They are also correlated to the crossroads in the city in order to maintain a better fluency of the traffic.

Developed devices are easily integrated in the existing infrastructure, functioning in united network with wireless communication. They are flexible, modular and re-programmable and allow for fast and easy extending of functionality by user request for the solution of other tasks and adapt them to requirements and standards of different countries [8].

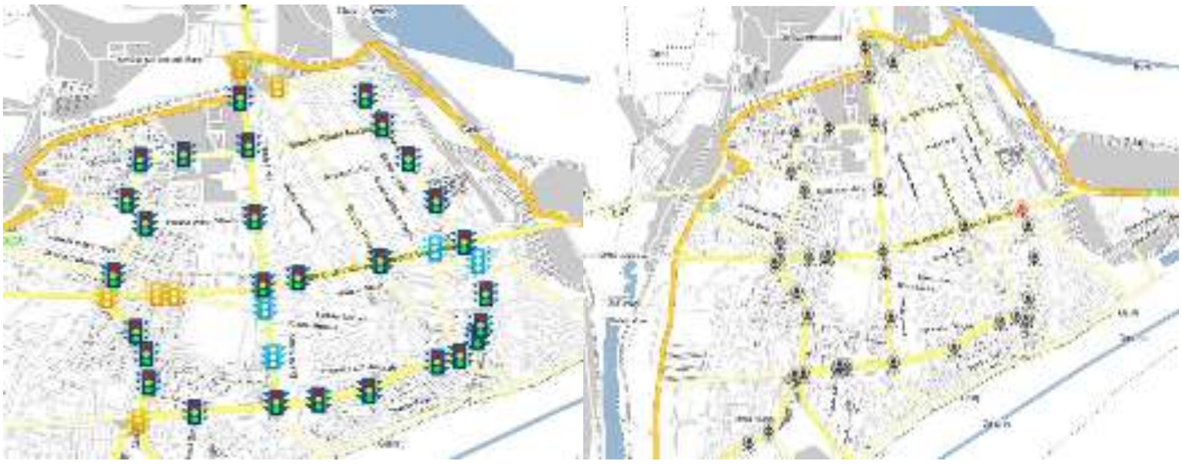

a) Traffic light controller

b) Automatic traffic surveillance system for vehicle tracking

Fig. 2. *Work Centre Utilization Report* [7]

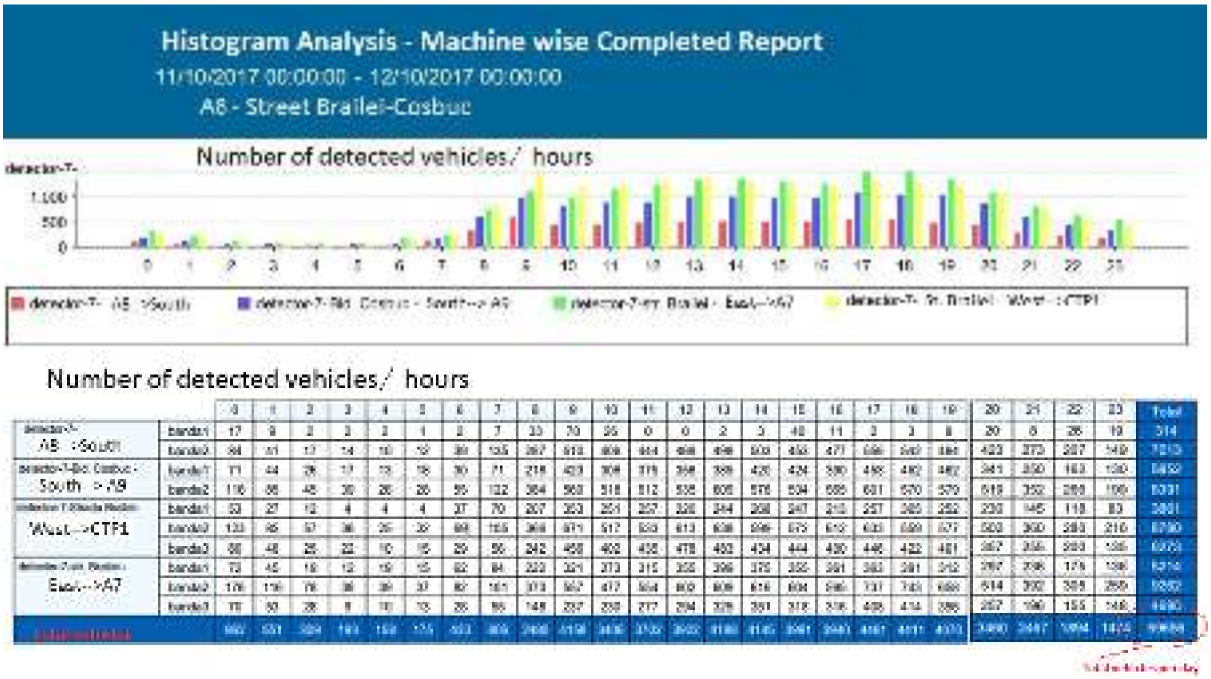

Fig. 3. *Machine wise Completed Report A8: Brailei – Cosbuc Street*

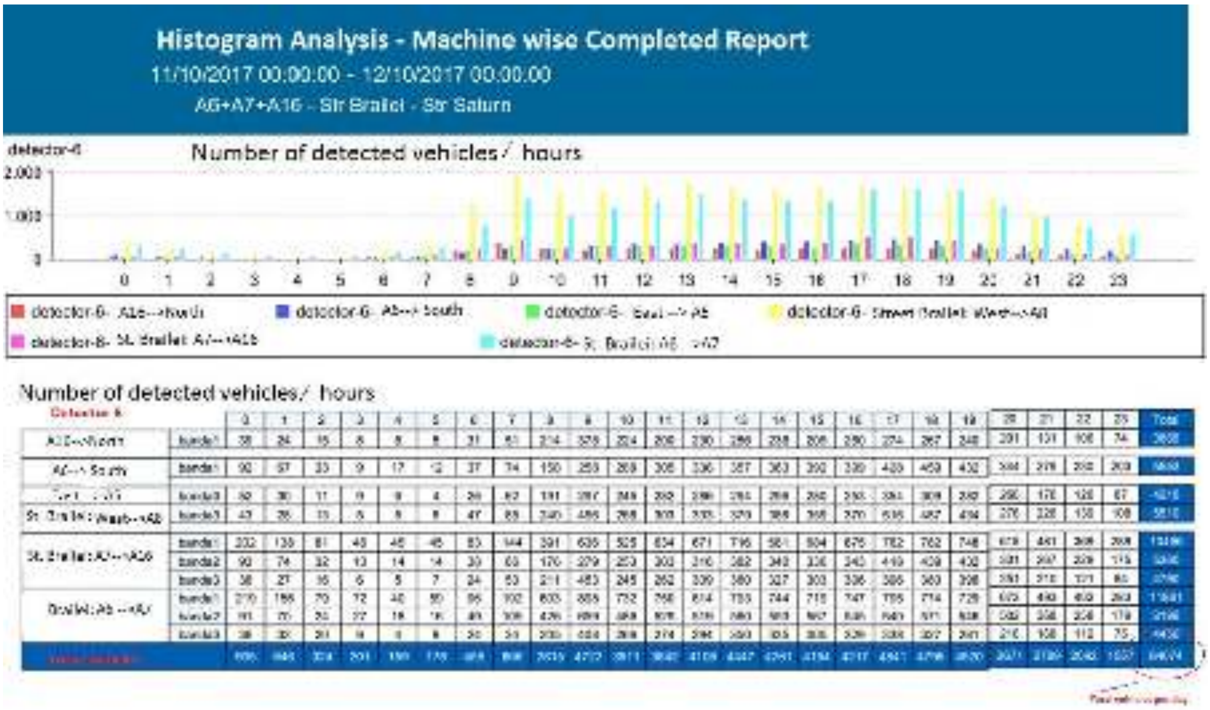

Fig. 4. *Machine wise Completed Report A8: Brailei – Cosbuc Street*

3.2. Negative impact of the traffic congestion

• Wasting time of drivers and passengers in blocked traffic affects the economic health of the nations. • Wasted fuel increases air pollution and carbon dioxide emission because of the increased idling, acceleration and braking.

• Due to blocked traffic, emergency vehicles may get delayed in reaching their destination where they are urgently needed.

• Spillover effect from congested main routes to secondary roads and side streets as alternative routes is attempted which affects the real estate prices.

• Delays may result in late arrival for employment, meetings and education, resulting in lost business, disciplinary action or other personal losses [4, 8].

4. How does the EU contribute to improving the quality of the urban environment?

Road traffic significantly affects the health of the population in overcrowded urban areas where traffic jams are formed. This is most obvious today when the chronic disease age remains a link between the health of the population and the environment.

People choose to live in urban areas so they can have a better quality of life. They want to be at the heart of economic activity, and to have more job opportunities and other social and economic advantages. However, city living brings a range of challenges. While living in close proximity to our daily activities can be more efficient and contributes to sustainability, other factors such as air pollution can be far more acute in cities.

Overcrowding, traffic pollution, noise, and industrial emissions are just a few of the issues that have to be constantly monitored and addressed to achieve a high quality of life without high environmental costs. But doing this will also bring benefits beyond city borders.

The Urban Environment is important for all of us, because so many of us live in cities. The European Commission recognizes the role that cities play in the lives of so many Europeans and has committed itself to act in this area. Urban environments directly influence the lives of millions of European citizens and, in turn, have a substantial impact on the wider environment. European cities need more than ever to be sustainable and should offer the kind of quality of life and opportunity that make people want to live there and make businesses want to invest [9].

4.1. The EU and the urban environment

Key elements of the EU's approach to the urban environment [10]:

1. The Thematic Strategy on the Urban Environment aims for better implementation of the

existing EU environmental policies and legislation at local level through the exchange of experience and good practice between Europe's local authorities, in order to achieve 'a better quality of life through an integrated approach concentrating on urban areas.' Its principles and approaches are reflected further in other strategies such as the Thematic Strategy on Air Pollution.

2. The Leipzig Charter on Sustainable European Cities demonstrates a further commitment to making our cities healthy, attractive and sustainable places to live and work in.

3. The renewed Sustainable Development Strategy for the EU calls for the creation of sustainable local communities with a high quality of life, attention to urban transport and greater cooperation between urban and rural areas.

4. The renewed Lisbon Strategy sets as a priority the high quality of urban environments to 'make Europe a more attractive place in which to invest'.

5. The Europe 2020 Strategy builds on the Lisbon Strategy and sets out a broader approach aimed at achieving a resource efficient Europe. This means decoupling economic growth from the use of resources, supporting the shift towards a low carbon economy, increasing the use of renewable energy sources, modernizing our transport sector and promoting energy efficiency – actions that will affect the cities of Europe.

5. Conclusions

The importance of road transport in the Union's transport policy is also highlighted by the share of this mode of transport in both freight and passenger transport. Cities make up only two percent of the earth's surface, yet they are home to over half of the world's population. In Europe, the proportion of urban dwellers is even higher. Today, nearly 75% of Europeans live in cities and urban areas, and by 2020 this is expected to rise to 80%.

In the light of these considerations, the proposed work justifies its importance and usefulness in the field of traffic management in order to improve the quality of urban life.

We considered it useful to highlight the general objectives of EU policy in the transport sector, especially in metropolitan areas, where pollution is expected to increase, as a consequence of increased vehicle purchases.

EU legislation on road transport must be adopted taking into account social, technical, tax, safety and environmental regulations. That is why road transport regulations generally have the objective of providing a unitary framework for Member States in the field.

References

[1]. Chandra R., Mohan Rao A., Kanaga Durai B., Lakshmi S., *GIS Application in Traffic Congestion Management*, Proc. of Int. Conf. on Recent Trends in Transportation, Environmental and Civil Engineering, p. 66, 2011.

[2]. Harvey J. Miller, *GIS based dynamic traffic congestion modelling to support time-critical logistics*, Department of Economics, University of Alberta, Canada, 1999.

[3]. McNally M. G., Marca J. E., Rindt C. R., Koos A. M., *GPS/GIS Technologies for Traffic Surveillance and Management*, Institute of Transportation Studies and Department of Civil & Environmental Engineering, 2002.

[4]. ***, https://ortus.rtu.lv/science/en/innovations/20.

[5]. Mala S. P. Varma, *Minimization of Traffic Congestion by Using Queueing Theory*, IOSR Journal of Mathematics (IOSR-JM), vol. 12, issue 1, ver. II, p. 116-122, 2016.

[6]. Roger P. Roess, Elana S. Prassas, William R. McShane, *Traffic Engineering*, Third Edition, ISBN 0-13-142471-8.

[7]. ***, http://ro.uti.eu.com/index.php?pageid=1307&lang=ro.

[8]. Duranton Gilles, Turner Matthew A., *The Fundamental Law of Road Congestion: Evidence from U.S. Cities*. American Economic Review, 101, 6, p. 2616–2652, 2012.

[9]. ***, *Making our cities attractive and sustainable How the EU contributes to improving the urban environment*, Luxembourg: Publications Office of the European Union 2010, 36 p.

[10]. ***, http://ec.europa.eu/regional_policy.

FUEL CONSUMPTION STUDY FOR AUXILIARY ENGINES THAT EQUIP AN OIL TANKER

Mariana LUPCHIAN
“Dunarea de Jos” University of Galati, Romania
e-mail: mariana.lupchian@ugal.ro

ABSTRACT

The paper deals with an oil tanker whose propulsion system with internal combustion engine during navigation was investigated. For a power plant with internal combustion engines we distinguish the subsystems: the internal combustion engine; consumer (s); mechanisms and auxiliary installations of the internal combustion engine power plant. The energy required for the proper functioning of the energy system is provided by the engines it is equipped with. During the voyage, the ship has several conditions for navigation, and the main engine and auxiliary machinery do not work all the time on the same charge.

KEYWORDS: auxiliary machinery, fuel consumption, internal combustion engine, voyage, oil tanker

1. Introduction

The operating mode of the propulsion engine depends on: the type of ship, navigation conditions, ship body construction, propellant type, on the mode of transmission of energy from the engine to the propeller.

In the paper is calculated the fuel consumption of auxiliary engines that equip a ship.

The measurements were made on an oil tanker equipped with a single propeller.

2. Case study

We must take into account the fact that during a voyage the ship has more navigational situations and the main engine and auxiliary machinery do not always work at the same load.

The propulsion of the ship is provided by a six-cylinder MAN B & W Diesel Engine.

Engine power 9480 [kW], engine speed 127 [rpm]; ship speed 15.38 [Nd].

The ship is equipped with three Diesel generators, each of 6 cylinders in line 960 kW power, 900 rpm.

The main engine of a ship is the main fuel consumer and the major energy producer on board ships.

For a naval propulsion plant with internal combustion engines, an independent variable which gives its operating regimes is considered.

The study was conducted for several operating modes for full load and ballast. Ballast tanks are built into the hull of a ship in order to help maintain its stability by filling them with seawater.

We calculated the fuel consumption for auxiliary engines for each navigation situation (a. ship's march; b. loading the ship; c. maneuvers through straits; d. stationary with loading; e. stationary with unloading) [1].

a. $$P_{MA,1} = \mu_{MA,1} \cdot P_{e,MA} \cdot 2 \text{ [kW]} \quad (1)$$

- $\mu_{MA,1}$ = 0.47 - the charge coefficient of the auxiliary motors;

$$\dot{m}_{MA,C,1} = P_{MA,1} \cdot CS_{MA,C} \text{ [kg/h]} \quad (2)$$

- $\dot{m}_{MA,C,1}$ - fuel consumption of auxiliary engines

- $CS_{MA,C}$ - specific fuel consumption of auxiliary motors = 0.180 [kg / kW.h] [5]

$$\tau_{MA,m,1} = \tau_{m,7} + \tau_{b,3} \text{ [h]} \quad (3)$$

$\tau_{m,7}$ - the time of march to the port of origin;

$\tau_{b,3}$ - the march time to the destination port;

$\tau_{MA,m,1}$ - the number of engine operating hours;

$$CC_{MA,1} = \dot{m}_{MA,C,1} \cdot \tau_{MA,m,1} \cdot 10^{-3} \text{ [t]} \quad (4)$$

$CC_{MA,1}$ - fuel consumption of auxiliary engines;

b. $$P_{MA,2} = \mu_{MA,2} \cdot P_{e,MA} \cdot 2 \text{ [kW]} \quad (5)$$

$\mu_{MA,2}$ = 0.495 - the charge coefficient of the auxiliary motors;

$$\dot{m}_{MA,C,2} = P_{MA,2} \cdot CS_{MA,C} \text{ [kg/h]} \quad (6)$$

$\dot{m}_{MA,C,2}$ - hourly fuel consumption of auxiliary engines;

$$\tau_{MA,m,2} = \tau_{m,i} + \tau_{b,i} \text{ [h]} \quad (7)$$

$\tau_{MA,m,2}$ - the number of operating hours of the auxiliary motors;
$\tau_{m,i}$ - running time of auxiliary engines (full load);
$\tau_{b,i}$ - operating time of auxiliary motors (ballast);

$$CC_{MA,2} = \dot{m}_{MA,C,2} \cdot \tau_{MA,m,2} \cdot 10^{-3} \text{ [t]} \quad (8)$$

$CC_{MA,2}$ - fuel consumption of auxiliary engines (freight loading march);

c. $$P_{MA,3} = \mu_{MA,3} \cdot P_{e,MA} \cdot 2 \text{ [kW]} \quad (9)$$

$\mu_{MA,3}$=0.625 - the charge coefficient of the auxiliary motors;

$$\dot{m}_{MA,C,3} = P_{MA,3} \cdot CS_{MA,C} \text{ [kg/h]} \quad (10)$$

$\dot{m}_{MA,C,3}$ - hourly fuel consumption of auxiliary engines;

$$\tau_{MA,m,3} = \tau_{m,s} + \tau_{b,s} \text{ [h]} \quad (11)$$

$\tau_{MA,m,3}$ - the number of operating hours of the auxiliary motors;
$\tau_{m,s}$ - running time of auxiliary engines (full load);
$\tau_{b,s}$ - running time of auxiliary engines (ballast) (maneuver through straits).

$$CC_{MA,3} = \dot{m}_{MA,C,3} \cdot \tau_{MA,m,3} \cdot 10^{-3} \text{ [t]} \quad (12)$$

$CC_{MA,3}$ - fuel consumption of auxiliary engines;

d. $$P_{MA,4} = \mu_{MA,4} \cdot P_{e,MA} \cdot 2 \text{ [kW]} \quad (13)$$

$\mu_{MA,4}$ - 0,420- the charge coefficient of the auxiliary motors;

$$\dot{m}_{MA,C,4} = P_{MA,4} \cdot CS_{MA,C} \text{ [kg/h]} \quad (14)$$

$\dot{m}_{MA,C,4}$ - fuel consumption of auxiliary engines;

$$\tau_{MA,m,4} = \tau_{m,6} + \tau_{b,2} \text{ [h]} \quad (15)$$

$\tau_{MA,m,4}$ - the number of operating hours of the auxiliary motors;
$\tau_{m,6}$ - the loading time in the port of destination;
$\tau_{b,2}$ - the loading time in the port of origin;

$$CC_{MA,4} = \dot{m}_{MA,C,4} \cdot \tau_{MA,m,4} \cdot 10^{-3} \text{ [t]} \quad (16)$$

$CC_{MA,4}$ - fuel consumption of auxiliary engines;

e. $$P_{MA,5} = \mu_{MA,5} \cdot P_{e,MA} \cdot 2 \text{ [kW]} \quad (17)$$

$\mu_{MA,5}$ = 0.8 - the charge coefficient of the auxiliary motors;

$$\dot{m}_{MA,C,5} = P_{MA,5} \cdot CS_{MA,C} \text{ [kg/h]} \quad (18)$$

$\dot{m}_{MA,C,5}$ - fuel consumption of auxiliary engines;

$$\tau_{MA,m,5} = \tau_{m,5} + \tau_{b,8} \text{ [h]} \quad (19)$$

$\tau_{m,5}$ - download time in the port of destination;

$\tau_{b,8}$ - download time in the port of origin;

$\tau_{MA,m,5}$ - the number of operating hours of the auxiliary motors;

$$CC_{MA,5} = \dot{m}_{MA,C,5} \cdot \tau_{MA,m,5} \cdot 10^{-3} \text{ [h]} \quad (20)$$

$CC_{MA,5}$ - fuel consumption of auxiliary engines (stationary unloading);
$CS_{MA,C}$ - specific fuel consumption of auxiliary engines = 0.180 [kg/kW.h];

Fuel consumption of auxiliary engines on voyage:

$$CC_{MA,total} = CC_{MA,1}+CC_{MA,2}+CC_{MA,3}+CC_{MA,4}+CC_{MA,5} \quad (21)$$

Fuel consumption of auxiliary engines (annual):

$$CC_{MA,total,an} = CC_{MA,total} \cdot N_{v} \quad (22)$$

The calculations were made based on a program in Engineering Equation Solver.

Figure 1 shows the ship's speed (load and ballast). In Table 1 are presented the results obtained for the fuel consumption of auxiliary machines for several navigation situations.

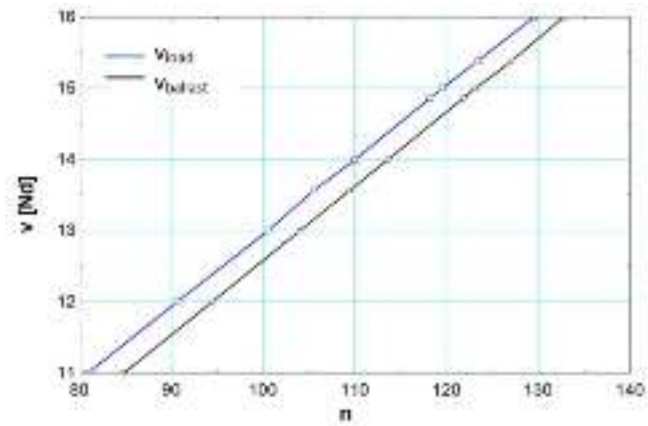

Fig. 1. *Speed of the ship*

Table 1. *Fuel consumption for the studied navigation situations*

Regime	CCMA;tot [t/voiaj]	CCMA,1 [t]	CCMA,2 [t]	CCMA,3 [t]	CCMA,4 [t]	CCMA,5 [t]
regime 1	98,870	85,390	2,737	2,592	2,423	5,722
regime 2	97,990	84,520	2,737	2,592	2,423	5,722
regime 3	93,175	79,700	2,738	2,592	2,423	5,722

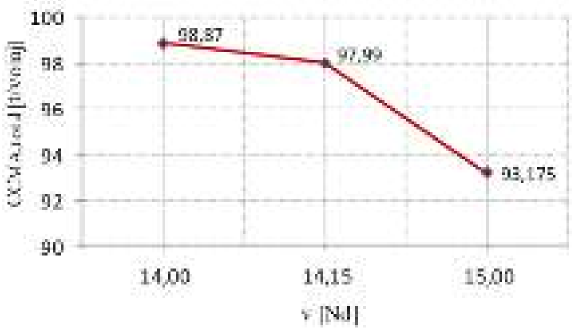

Fig. 2. *Fuel consumption*

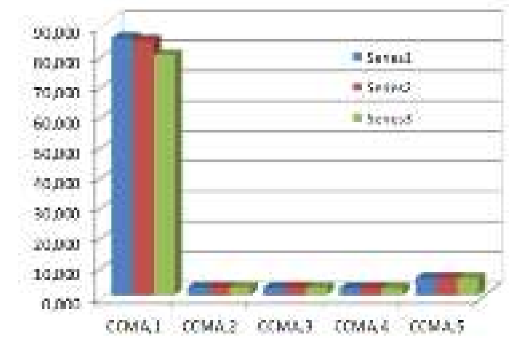

Fig. 3. *Fuel consumption for the studied navigation situations*

3. Conclusions

The fuel consumption of the auxiliary engines is the lowest for operating at speed v = 150 [Nd].

For the operating mode with: speed of the ballast ship vb = 15 Nd, the fuel consumption is: CCMA, total = 93,175 [t/voyage]. The calculations were made based on a program in Engineering Equation Solver.

The vessel must operate at the parameters for which it was designed and built, thus meeting all technical and economic requirements.

References

[1]. Lupchian Mariana, *Analysis of the operating regimes of power plants for different situations naval navigation*, SECTION I – Navigation and Maritime Transport, Constanţa Maritime University Annals, vol. 19, p. 51, Editura Nautica, 2013.

[2]. Lupchian Mariana, *The profit made by a oil tanker after a voyage*, CIEI 2011, The 8th International Conference On Industrial Power Engineering, Aprilie 14-25, ISSN-L 2069-9905, Bacău, 2011.

[3]. Simionov Mihai, *Instalaţii de propulsie navale. Linii de arbori*, Editura Evrika, Brăila, 2001.

[4]. ***, *The Motor Ship, Waste management is a grey area for owners*, 2001.

[5]. Simionov M., *Instalaţii de propulsie navală*, Galati University Press, 2009.

[6]. Ceangă V., Mocanu C. I., Teodorescu C., *Dinamica sistemelor de propulsie*, Editura Didactică şi Pedagogică, Bucuresti, 2003.

THE ANNALS OF "DUNAREA DE JOS" UNIVERSITY OF GALATI
FASCICLE IX. METALLURGY AND MATERIALS SCIENCE
N°. 2 - 2017, ISSN 1453-083X

Ni-P COATING ON STEEL SUPPORT BY ELECTROLESS METHOD

Tamara RADU, Andreea Georgiana DOBREA
"Dunarea de Jos" University of Galati
e-mail: tradu@ugal.ro

ABSTRACT

The autocatalytic reduction method (electroless method) was applied to obtain the Ni-P layers with different P contents. Nickel sulfate was used as nickel ion source and as reducing agent the sodium hypophosphite. The surface morphology, microstructure, layers thickness and corrosion resistance in acidic and basic environment were analyzed. The research results show a strong connection between layer characteristics and process parameters: pH and temperature. The analyzed layers show a high stability in 10% NaOH solution and different corrosion rates in HCl solutions (1 N and 0.5 N) depending on the phosphorus content in the layer.

KEYWORDS: Ni-P alloys, macrostructure, microstructure, corrosion resistance

1. Introduction

The electroless deposition method consists of the immersion of the support in a solution containing, in principle, a salt for providing the ions of the metal to be deposited and a reducing agent. Several metals and alloys can be deposited through this method, such as: Sn, Cu, Mn, Co, Ni-P, Ni-B, Ni-P-Sn, Ni-P-Zn: and others, on different supports: steel, Al, Mg, Cu, *et all*. The name of the method comes from the fact that no external electrical source is used. When Ni-P alloys layers are obtained, the solution contains $NiSO_4$ or NiCl and the reduction is done with sodium hypophosphite. By using hypophosphite ions as a reducing agent, the reactions underlying the deposition of Ni-P on the active surface of the support are the following [1]:

$$Ni^{2+} + H_2PO_2^- + H_2O \rightarrow Ni + 2H^+ + H(HPO_3)^- \quad (1)$$

$$HPO_2^- + H_2O \rightarrow H(HPO_3)^- + 1/2H_2 \quad (2)$$

When using sodium hypophosphite, Ni-P coatings with phosphorus in varying concentrations are obtained, from 1 to 12%, depending on the process parameters. The phosphorus content is very important as it determines the structure and consequently the properties of the coating [2-4]. Ni-P layers with low-phosphorus have a high resistance to wear that can be improved by heat treatment [5-7]. High P content in the layer grants high corrosion resistance [8-10]. The method also has the advantage of covering supports with complicated configurations because the deposited layer closely follows the topography of the surface [11].

Many of the reactions from the electroless process are sensitive to the changes in the solution pH. The main nickel reduction reaction is accelerated by the increase of the pH and, since it predominantly controls the deposition rate, increasing the pH of the solution leads to an increase in the nickel deposition rate. At the same time, the increase of the solution pH leads to a slowdown in phosphorus reduction due to the production of hydroxide ions. Therefore, increasing the solution pH leads to decreases in the phosphorus content of the coating. To maintain the pH at the desired values in the coating solution, a buffering agent is inserted. Specialty literature indicates a wide range of such substances [12]. The solution may also contain other additives that improve the stability and the characteristics of the deposited layer [13]. This paper shows the way to obtain Ni-P alloy layers, with different phosphorus content, by electroless method using a simple and accessible solution that can also be applied industrially.

2. Experimental conditions

The bath used to obtain Ni-P layers contains the following salts:

- nickel sulphate, as a supplier of nickel ions - 25 g/L;
- sodium hypophosphite, as reducing agent - 23 g/L;
- sodium acetate, as complexing and buffering agent - 9 g/L;
- lead acetate, as a stabilizer by lead ions - 0.01 g/L.

The salts were dissolved in distilled water and placed in the bath of the experimental installation, charged with 0.5 L distilled water at 70 °C, in the following order: lead acetate, sodium acetate, nickel sulfate and sodium hypophosphite.

After the salts were introduced, the bath was filled with distilled water up to the work volume (1 L) and the solution was stirred at 300 rpm. The working temperature was 83 °C and pH 6.6; 5.11 and 4.32. The pH was corrected with glacial acetic acid or ammonium hydroxide, as appropriate. The cleaning of the surface of steel strips samples had three operations:

- cleaning in commercial solution (MASCO) at pH = 2 and 60 ºC; immersion time 3 min;
- washing in hot water at 60 ºC;
- washing in hot water at 80 ºC.

3. Characterization of layers

For the characterization of the samples, specific analyses were made to determine the main characteristics of practical interest, namely:

- chemical and structural analysis;
- layer thickness;
- corrosion behavior.

3.1. Chemical composition

The chemical composition was determined by EDX analysis on an electron microscope, Quanta 200 type, equipped with an X-ray analyzer. The analysis was performed in layers section, obtained at the three experimental pH values (4.3, 5.11, 6.6) at a 5 minutes immersion time, at 83 ºC. EDX spectra show an increase of phosphorus content to at lower pH. Figure 1 shows the result of EDX analysis on a Ni-P layer obtained at pH = 5.11. The diffraction spectrum presents, alongside Ni and P, peaks for Fe, C and O. Fe and C come from the steel support and O occurs as a result of surface oxidation. The chemical analysis showed phosphorus contents from 4.74 (pH = 6.6) to 12.42 wt.% (pH = 4.3). At pH = 5.11 the phosphorus contents were 9.53 wt.%.

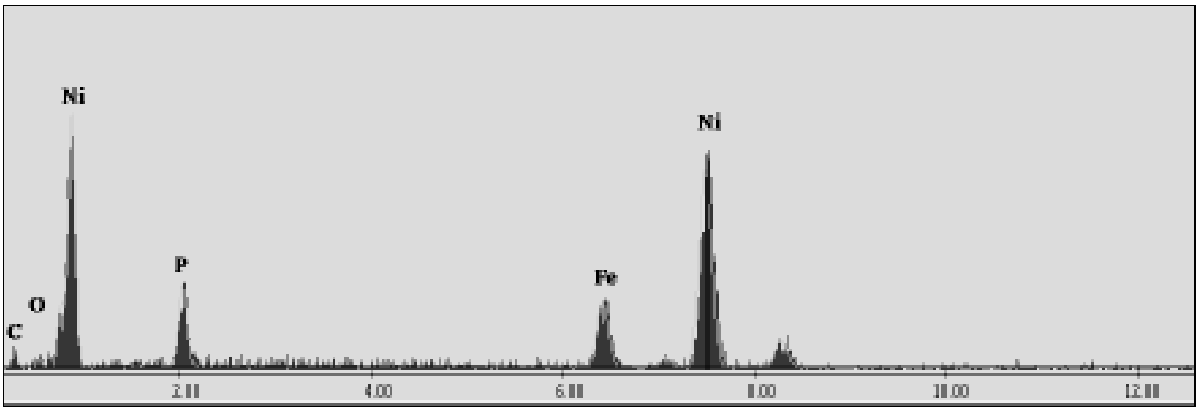

Fig. 1. *EDS spectra for the Ni-P layers obtained at pH = 5.11 and 5 min immersion time, at 83 ºC*

3.2. Surface morphology

The macroscopic surface of the Ni-P coated strips has a very glossy and smooth silvery look. Microscopically (Fig. 2, a, b, c), regardless of the experimental conditions, a strip deposit is observed which closely follows the roughness of the steel substrates. Moreover, an increase in the layer’s uniformity is observed, at decreasing the pH, without having the substrate roughness completely disappear. (Fig. 2c).

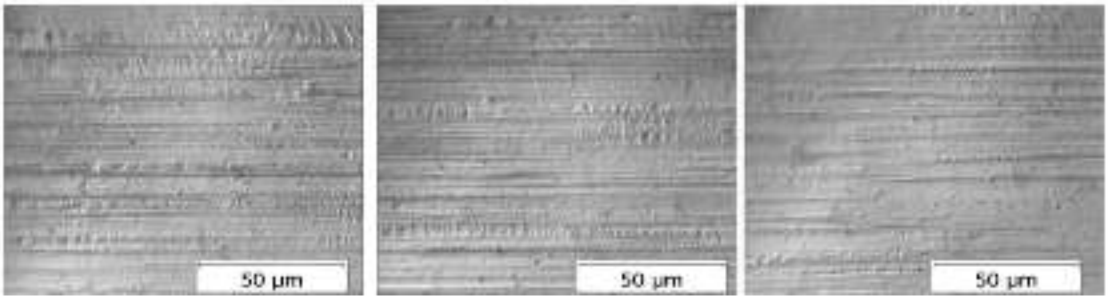

Fig. 2. *Optical micrographs of Ni-P layer depending on the pH, T = 83 °C, 5 min.*

3.3. Layer thickness

The layer thickness is a challenge in the electroless coating method. The deposition is relatively slow and, only when the optimum parameters are assured, a thickness over 20 μm can be obtained. Out of these parameters, the immersion time is important but also the temperature and pH. In order to ensure high productivity, the nickel-plating process requires a reduced duration, a high working temperature and an acidic pH. In order to analyze the effect of the considered working parameters on the thickness of the layer, the metallographic measurement method was applied. In Figure 3 a, b the optical thicknesses are presented, measured on the optical microscope, which were obtained at immersion times of 5 minutes at 83 °C at the three experimental pHs. There is a decrease in layer thickness from 5 μm to 2 μm, when the pH decreases.

For the electroless process, the nickel deposition rate increases exponentially at temperature rise, the variation curve being similar to other deposition techniques (Fig. 4).

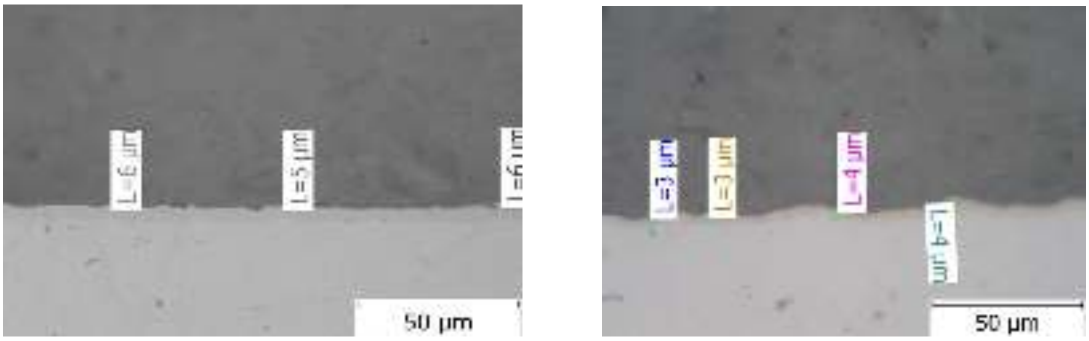

a) pH-6.6 b) pH-4.32

Fig. 3. *Influence of the pH on layer thickness*

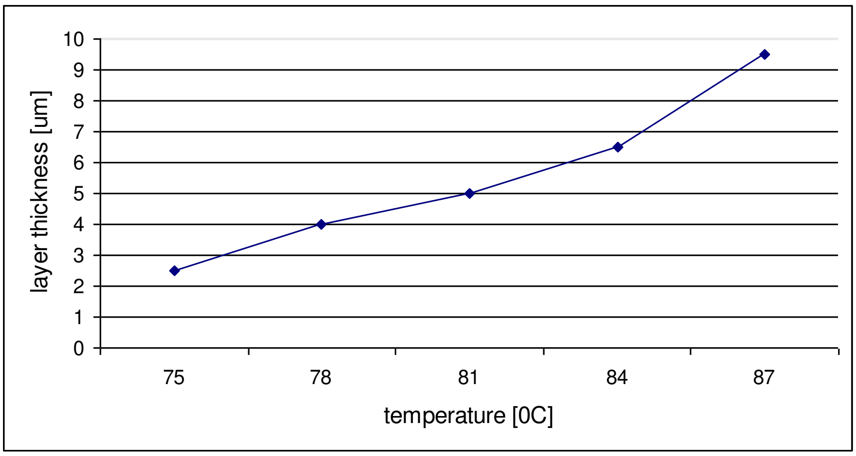

Fig. 4. *Influence of the temperature on layer thickness*

The deposition rate is low at temperatures below 75 °C and increases with temperature increase [14]. Generally, in the nickel electroless process the maximum working temperature is about 90 °C. Above this temperature the bath tends to become unstable.

3.4. Corrosion resistance

The corrosion resistance evaluation was done in various corrosive environments by gravimetric method, according to G1 / 2004.

The following steps were taken:

- weighing with four decimals of the samples, resulting in the initial mass;
- immersion in crystallizers, where the corrosive environment is;
- removing samples after a determined time and washing them with distilled water to remove corrosion products and then with acetone followed by drying;
- weighing dry samples.

Samples were selected with different phosphorus contents (small, medium, high) obtained at different pH values coded according to Table 1.

***Table 1.** Samples tested*

Code	Layer types and conditions of obtaining
NP1	layer Ni-P with small phosphorus (4.47 wt.% P), obtained at pH-6.60, 83 °C, 5 min.
NP2	layer Ni-P with medium phosphorus (9.53 wt.% P), obtained at: pH-5.11, 83 °C, 5 min.
NP3	layer Ni-P with high phosphorus (12.42 wt.% P), obtained at: pH-4.32, 83 °C, 5 min.

These samples were individually submerged, according to G31 / 2004, in containers containing 1 N and 0.5 N hydrochloric acid solution. Samples were weighed to determine the initial mass and measured for surface determination.

The study was conducted over a period of 168 hours (one week) For the calculation of the corrosion rate, the following relation was applied:

$$v_{cor} = \frac{m_{cor}}{S \cdot t}$$

where:

v_{cor} - gravimetric index [g/m^2·h];

m_{cor} - mass loss by corrosion [g];

S - surface area of the samples [m^2];

t - corrosion time [h].

3.4.1. Corrosion behavior estimation, in corrosive environment 1 N HCl

For each type of layer, the corrosion rate in 1 N hydrochloric acid was determined as average on samples subjected to corrosion (minimum three per coating type). The results after 168 hours are presented in Figure 5. As it can be seen from this data, the sample with a medium phosphorus content (Vcor = 1.35) has the best corrosion behavior in this highly corrosive medium and the sample with lower phosphorus content (Vcor = 2.60) the weakest behavior.

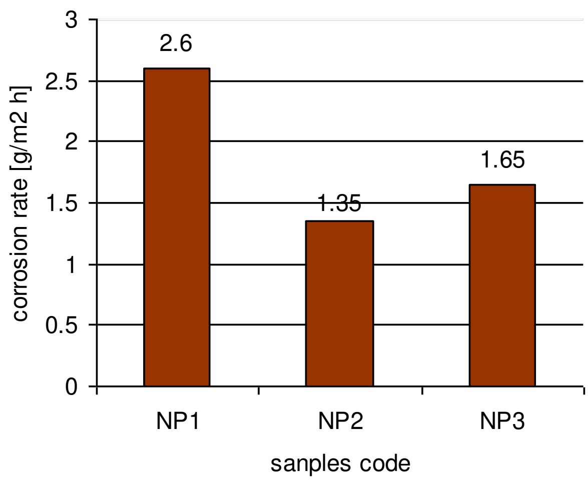

***Fig. 5.** Corrosion rate in 1 N HCl depending on the type of protection layer, after 168 hours of testing*

The direct observation of the samples, after 168 hours of corrosive attack, showed an attenuation of the metallic gloss for all samples. Moreover, on all samples were localized attacks with the formation of red rust spots. Figure 6 shows aspects of the surface of highly corroded samples.

Localized corrosion is specific to nickel coatings because it provides a cathodic protection to the steel support, so any porosity or nonuniformity of the layer will result in a strong corrosive effect of the steel substrate. The localized corrosive attacks observed on samples may also be caused by microscopic defects such as micro-porosity or discontinuity of the layer due to the presence of impurities anchored from the nickel bath as shown in Figure 7.

The initial appearance of the surface

Sample code NP1

Sample code NP2

Sample code NP3

Fig. 6. *Macroscopic appearance of Ni-P layers after corrosive attack in 1 N HCl solution, 1:1*

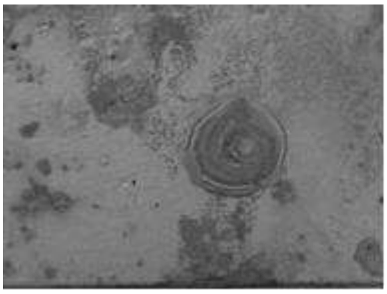

Fig. 7. *Localized corrosion caused by a pore, 1:1*

3.4.2. Corrosion behavior in corrosive environment 0.5 N HCl

The results of the corrosion process after 168 hours in 0.5 N HCl are shown in Figure 8. The sample with high phosphorus content (Vcor = 0.43) has the best corrosion behavior in this corrosive environment and the sample with medium phosphorus content (Vcor = 2.64) has the highest corrosion rate.

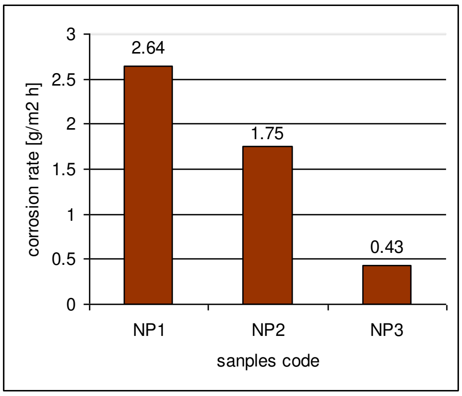

Fig. 8. *Corrosion rate in 0.5 N HCl depending on the type of protection layer, after 168 hours of testing*

Macroscopic analysis (with the naked eye and magnifying glass X20) shows the production of generalized corrosion, with the formation of a smaller amount of corrosion products than the previous test.

3.4.3. Assessment of corrosion resistance in the basic environment

The basic environment in which the samples were individually immersed was 10% NaOH solution. They were kept for 1.512 hours, every 168 hours being removed, washed, dried and weighed. As it can be seen in Table 4, mass loss is zero or within the range of 0.0001-0.0003 (within the error limit), which means zero corrosion rate in 10% NaOH. All types of coatings tested proved to be practically inert in the alkaline medium during the experiment.

Table 4. *Test results in 10% NaOH solution*

Sample mass	NP1	NP2	NP3
m_0 (initial)	0.7866	1.3432	3.9313
m_1 (after168 hours)	0.7866	1.3434	3.9315
m_2 (after 336 hours)	0.7867	1.3433	3.9314
m_3 (after 504 hours)	0.7866	1.3432	3.9315
m_4 (after 672 hours)	0.7866	1.3433	3.9313
m_5 (after 840 hours)	0.7865	1.3433	3.9314
m_6 (after 1008 hours)	0.7868	1.3437	3.9313
m_7 (after 1176 hours)	0.7864	1.3433	3.9314
m_8 (after 1344 hours)	0.7865	1.3436	3.9316
m_9 (after 1512 hours)	0.7868	1.3433	3.9313

4. Conclusions

Ni-P alloy layers with different phosphorus content obtained by electroless method used a simple and approachable solution: nickel sulfate 25 g/L, sodium hypophosphite 23 g/L, lead acetate 0.01 g/L and sodium acetate 9 g/L.

The surface of the Ni-P layers obtained has a very glossy and smooth silver look with an increase of the uniformity at pH decrease.

It is observed a decrease in layer thickness from 5 μm to 2 μm when the pH decreased from 6.6 to 4.32;

The sample with 9.53 phosphorus content (Vcor = 1.35) has the best corrosion behavior in 1 N hydrochloric acid (after 168 hours of testing) and the sample with 4.47 phosphorus content (Vcor = 2.60) has the weakest corrosion behavior.

All types of coatings tested proved to be practically inert in the alkaline medium during the experiment (1512 hours).

References

[1]. Krishnan K. H., John S., Srinivasan K. N., Praveen J., Ganesan M., Kavimani P. M., *An Overall Aspect of Electroless Ni-P Depositions - A Review Article*, Metallurgical and Materials Transactions A, vol. 37A, June 2006.

[2]. ***, *Quality Metal Finishing guide. Electroless Nickel Plating*, vol. 1, no. 5, http://infohouse.p2ric.org/ref/25/24301.pdf.

[3]. Mallory O. G., Hajdu J. B., *Electroless Plating: Fundamentals and Applications*, sponsored and published by American Electroplaters and Surface Finishers Society, 1990.

[4]. Khim Myo, *Effects of surfactants on characteristics and applications of electroless nickel-phosphorous deposits*, chapter 2 of thesis master of engineering, 2003.

[5]. Balint S. I., Constantinescu S., Balint L., *Influence of heat treatment on the characteristics of Ni-P-Al_2O_3 composite layers*, 15th International Multidisciplinary Scientific GeoConference SGEM 2015, Conference Proceedings, book 6, vol. 1, p. 99-111, 2015.

[6]. Balint L., Ciocan A., Balint S. I., Alexandru P., *The effect of heat treatment on the structure and characteristics of electroless Ni-P layer*, 16th International Multidisciplinary Scientific GeoConference, SGEM 2016, Albena, Bulgaria, Conference Proceedings, book 6, vol. 1, p. 345-352, 2016.

[7]. Lucica Balint, Gina Genoveva Istrate, *Caracterisation Ni-P and composite Ni-P-Al_2O_3 electroless layers*, Proceeding UGALMAT 2016.

[8]. Gina Genoveva Istrate, Tamara Radu, *Corrosion Behavior of Ni-P Coated Steel Strips*, The Annals of "Dunarea de Jos" University of Galati. fascicle IX. Metallurgy and Materials Science. no. 3, p. 48-52, 2015.

[9]. Radu T., Vlad M., Potecasu F., Istrate G. G., *Preparation and characterisation of electroless Ni-P-Al_2O_3 nanocomposite coatings*, Digest Journal of Nanomaterials and Biostructures, vol. 10, no. 3, p. 1055-1065, 2015.

[10]. Sankara Narayanan T. S. N., Baskaran I., Krishnaveni K., Parthiban S., *Deposition of electroless Ni-P graded coatings and evaluation of their corrosion resistance*, Surface & Coatings Technology 200, p. 3438-3445, 2006.

[11]. Florentina Potecasu, Tamara Radu, *The Influence of the Steel's Surface Quality on the Electroless Ni-P Coatings*, The

Annals of “Dunarea de Jos” University of Galati. fascicle IX. Metallurgy and Materials Science, no. 1, p. 49-53, 2015.

[12]. Bielinski J., *The Role of Buffers and Coin Electroless Nickel Plating*, Oberflache Surface, vol 25, no. 12, p. 423-429, 1984.

[13]. Hari Krishnan K., John S., Srinivasan K. N., Praveen J., Ganesan M., Kavimani P. M., *An Overall Aspect of Electroless Ni-P Depositions-A Review Article*, Metallurgical and Materials Transactions A, volume 37A, p. 1917-1925, june 2006.

[14]. Istrate G. G., Balint S. I., Ciocan A., Dragan V., *Influence of technological parameters on layer thickness to obtain Ni-P electrolles coatings*, 15^{th} International Multidisciplinary Scientific GeoConference SGEM 2015, www.sgem.org, SGEM2015 Conference Proceedings, ISBN 978-619-7105-42-1 / ISSN 1314-2704, book 6, vol. 1, p. 113-125, June 18-24, 2015.

MANUSCRISELE, CĂRŢILE ŞI REVISTELE PENTRU SCHIMB, PRECUM ŞI ORICE CORESPONDENŢE SE VOR TRIMITE PE ADRESA:

MANUSCRIPTS, REVIEWS AND BOOKS FOR EXCHANGE COOPERATION, AS WELL AS ANY CORRESPONDANCE WILL BE MAILED TO:

LES MANUSCRIPTS, LES REVUES ET LES LIVRES POUR L'ECHANGE, TOUT AUSSI QUE LA CORRESPONDANCE SERONT ENVOYES A L'ADRESSE:

MANUSCKRIPTEN, ZIETSCHRITFTEN UND BUCHER FUR AUSTAUCH SOWIE DIE KORRESPONDENZ SID AN FOLGENDE ANSCHRIFT ZU SEDEN:

After the latest evaluation of the journals by the National Center for Science Policy and Scientometrics (**CENAPOSS**), in recognition of its quality and impact at national level, the journal will be included in the B^+ category, 215 code (http://cncsis.gov.ro/userfiles/file/CENAPOSS/Bplus_2011.pdf).

The journal is already indexed in:

SCIPIO-RO: http://www.scipio.ro/web/182206

EBSCO: http://www.ebscohost.com/titleLists/a9h-journals.pdf

Google Academic: https://scholar.google.ro

The papers published in this journal can be viewed on the website of "Dunarea de Jos" University of Galati, the Faculty of Engineering, pages: http://www.sim.ugal.ro, http://www.imsi.ugal.ro/Annals.html.

Name and Address of Publisher:
Contact person: Elena MEREUȚĂ
Galati University Press - GUP
47 Domneasca St., 800008 - Galati, Romania
Phone: +40 336 130139
Fax: +40 236 461353
Email: gup@ugal.ro

Name and Address of Editor:
Prof. Dr. Eng. Marian BORDEI
Dunarea de Jos University of Galati, Faculty of Engineering
111 Domneasca St., 800201 - Galati, Romania
Phone: +40 336 130208
Phone/Fax: +40 336 130283
Email: mbordei@ugal.ro

AFFILIATED WITH:
- THE ROMANIAN SOCIETY FOR METALLURGY
- THE ROMANIAN SOCIETY FOR CHEMISTRY
- THE ROMANIAN SOCIETY FOR BIOMATERIALS
- THE ROMANIAN TECHNICAL FOUNDRY SOCIETY
- THE MATERIALS INFORMATION SOCIETY
(ASM INTERNATIONAL)

Edited under the care of
the FACULTY OF ENGINEERING
Annual subscription (4 issues per year)

Editing date: 15.06.2017
Number of issues: 200
Printed by Galati University Press (accredited by CNCSIS)
47 Domneasca Street, 800008, Galati, Romania